DOKUZ EYLÜL UNIVERSITY GRADUATE SCHOOL OF NATURAL AND APPLIED SCIENCES

EXPERIMENTAL AND ANALYTICAL WORK ON THE SEISMIC PERFORMANCE OF DIFFERENT TYPES OF MASONRY INFILLED REINFORCED CONCRETE FRAMES UNDER CYCLIC LOADING

by

Ali A. WALY

August, 2010

İZMİR

EXPERIMENTAL AND ANALYTICAL WORK ON THE SEISMIC PERFORMANCE OF DIFFERENT TYPES OF MASONRY INFILLED REINFORCED CONCRETE FRAMES UNDER CYCLIC LOADING

A Thesis Submitted to the

Graduate School of Natural and Applied Sciences of Dokuz Eylül University In Partial Fulfillment of the Requirements for the Degree of Master of Science in Structural Engineering.

by

Ali A. WALY

August, 2010

İZMİR

M.Sc THESIS EXAMINATION RESULT FORM

We have read the thesis entitled **"EXPERIMENTAL AND ANALYTICAL WORK ON THE SEISMIC PERFORMANCE OF DIFFERENT TYPES OF MASONRY INFILLED REINFORCED CONCRETE FRAMES UNDER CYCLIC LOADING"** completed by **ALI A. WALY** under supervision of **PROFESSOR SERAP KAHRAMAN** and we certify that in our opinion it is fully adequate, in scope and in quality, as a thesis for the degree of Master of Science.

.....
Prof. Dr. Serap KAHRAMAN

Supervisor

....

(Jury Member) (Jury Member)

.....

Prof.Dr. Mustafa SABUNCU
Director

Graduate School of Natural and Applied Sciences

ACKNOWLEDGEMENTS

I would like to express my great admiration and send my special thanks to my supervisor Prof. Dr. Serap KAHRAMAN for her precious patience, guidance and effort of teaching desire throughout my thesis and gradation. This thesis would not be completed without her supports.

I also would like to thank the other members of thesis committee Asst. Prof. Selçuk SAATÇI

I also would like to thank my tutors Asst. Prof. Özgür ÖZÇELİK, Serkan MISIR and Sadık Can GIRGIN for sharing their knowledge, providing me new information and for their guidance with OpenSees.

Finally, I give my special thanks to my family especially to my mother, my uncle Ibrahim ARAFAT and to all whom always being supporting me, for all their love and wonderful support throughout my master degree.

Ali A. WALY

EXPERIMENTAL AND ANALYTICAL WORK ON THE SEISMIC PERFORMANCE OF DIFFERENT TYPES OF MASONRY INFILLED REINFORCED CONCRETE FRAMES UNDER CYCLIC LOADING

ABSTRACT

Structural frame buildings with masonry infilled walls make up a significant portion of the buildings so it is very important to understand the behavior of masonry especially under earthquake effect. This thesis presents an experimental work and analytical modeling of reinforced concrete frame infilled with different types of masonry clay bricks and subjected to slowly applied cyclic lateral loads.

Two different types of clay bricks are considered in this study, in order to understand the effect of masonry wall on the whole system under lateral cyclic load. An OpenSees model of the frame is used to simulate the experimental work carried out in Dokuz Eylul University, Civil Engineering Department, Structural Mechanics and Earthquake Engineering Laboratory by using OpenSees.

In this study two equivalent diagonal struts are developed in OpenSees to model infill masonry wall. The effects of number of bay and the effects of the soft storey mechanism studied with the calibrated analytical model. The results obtained from the experimental and analytical work show the significance of infill in increasing the strength and lateral stiffness of the entire system under lateral load, which is a faction of type of clay brick used.

Keywords: Masonry infill, Reinforced concrete frame, Cyclic load, nonlinear finite element modeling, equivalent diagonal strut and soft story.

FARKLI TIP TUĞLA DOLGULU BETONARME ÇERÇEVELERIN TEKRARLI YÜK ALTINDAKI SISMIK PERFORMANSI ÜZERINE DENEYSEL VE ANALITIK ÇALIŞMA

ÖZ

Dolgu duvarlı çerçeve türü yapılar, yapıların önemli bir kısmını oluşturmaktadır; bu yüzden özellikle deprem etkisi altındaki dolgu duvar davranışının anlaşılması oldukça önemlidir. Bu tez çalışması kapsamında, farklı tipte dolgu duvar tuğlaları kullanılarak oluşturulan dolgu duvarlı maruz betonarme çerçevelerin yarı-statik (quasi-static) yükleme altında deneysel ve analitik olarak modellenmesi incelenmiştir.

Bu çalışmada, tersinir-tekrarlı yatay yük etkisi altında dolgu duvarın tüm taşıyıcı sistem davranışına etkisini anlamak için iki farklı tipte tuğla türü göz önüne alınmıştır. DEÜ İnşaat Mühendisliği Bölümü Yapı Mekaniği Laboratuarı'nda gerçekleştirilen deneysel çalışmaların benzeştirilebilmesi için Opensees Deprem Mühendisliği Simülasyon programı kullanılmıştır.

Bu çalışmada, dolgu duvarı iki adet eşdeğer diyagonal basınç çubuğu temsil etmektedir. Analitik çalışmada, çerçeve açıklığı ve yumuşak kat etkisi incelenmiştir. Deneysel ve analitik çalışmalardan elde edilen sonuçlar, dolgu duvarın yatay yük etkisi altında taşıyıcı sistemin bütününde, tuğla türünün karakteristiklerine bağlı olarak, dayanım ve yanal rijitliği arttırdığını göstermektedir.

Anahtar sözcükler : Dolgu duvar, betonarme çerçeve, tekrarlı yükleme, doğrusal olmayan sonlu elemanlar modellemesi, esdeğer dıyagonal eleman ve yumaşak kat mekanızması

CONTENTS

Page

CHAPTER ONE

INTRODUCTION

1.1 Introduction to Research

Recently, the most common structural system for both residential and office buildings consists of multi-level framed structures are masonry infilled RC frames so it is so important to determine the earthquake behavior of RC structures with infill walls under seismic load. Nonlinear structural analyses and finite element method are used to determine the earthquake behavior of structures with infill walls. For decades, nonlinear analyses and finite element method are getting improved and so many methods are developed in nonlinear structural analyses. Infilled frames have been investigated experimentally by many researchers (Mosalam, White and Gregely 2007 and Taher and Afefy 2008). Most of this effort has been focused on single-bay single-storey frames infilled with various materials and subjected to cyclic loading. Many researchers have realized the significant effects of the infilled masonry on the structural responses of frames. It yields that the presence of nonstructural masonry infill walls can affect the seismic behavior of framed building to large extent. These effects are generally positive: masonry infill walls can increase global stiffness and strength of the structure. On the other hand, potentially negative effects may occur such as torsional effects induced by in plan-irregularities, soft-storey effects induced by irregularities and short- column effects.

The infill walls are commonly seen in Turkey and it is very important to determine the effects of infill walls to structural behavior because Turkey is considered earthquake region so seismic load is so effective on structures located in region like Turkey.

In this study the seismic load can be defined as a testing procedure where cyclic loading is slowly applied to the tested structure. To understand the behavior of structures under earthquake investigations of the damages that occurring on specimens are considered. In this study bricks masonry infilled RC frames will be

tested and comparing its results with bare frame to understand the effect of the masonry panel well. The simulation part of structural response under cyclic load has been accomplished using the OpenSees analysis platform (http://opensees.berkeley.edu) developed as part of the Pacific Earthquake Engineering Research (PEER) Center research effort (http://peer.berkeley.edu) which we will be discussed it in section later.

1.2 Literature Review

A brief review of previous studies on infilled masonry reinforced concrete under seismic load is presented in this section.

Our first study of frame infilled with unreinforced masonry wall under seismic load by Mosalam, White and Gregely (1997). In their study, they treat an experimental investigation of gravity-load designed (GLD) frames, i.e., frames with semirigid connection, infilled with unreinforced masonry wall and subjected to slowly applied cyclic lateral loads. Various geometrical configurations of the frame and infill walls and different material types of the masonry walls are considered. Based on the results, a hysteresis model for infilled frames is formulated and discussed. In their study they focused on the performance of single-storey and they investigated the cracking behavior of the infill panel for reduced-scale infilled (GLD) frames under earthquake type loading and from this study it was found the effects of the following three primary parameters on the load deformation hysteretic behavior and on failure modes were investigated: (1) Number of bays; (2) material properties of the concrete blocks and mortar joints; and (3) type of infill openings. Mosalam mentioned in his study that the lateral application point was selected to preserve symmetry in the loading. Therefore, for two-bay specimens the applied load should apply at the top of the central column whereas for single-bay specimen, the load was applied at the midpoint of the top beam.

Bell and Davidson (2001) presented the evaluation of a reinforced concrete frame building with brick infill panels on the exterior walls. The evaluation uses an

equivalent strut approach for modeling the infill panels. Reference is made to international studies and guidelines, including FEMA-273 and Eurocode 8. In this study showed that the infill panels have the significant influence on the behavior of RC buildings in positive way. The reviewed sources in this study indicate that due to stiffness, strength, and damping effects of infill panels, deformations are below that required for a soft storey mechanism. Using ETABS analyses with an eccentric strut infill model carried this study out. The seismic performance of the building was assessed following the NZSEE and FEMA-273 guidelines. The evaluation showed the performance of the building to be satisfactory for the design earthquake.

Marjani and Ersoy (2002) submitted study investigated the behavior of the masonry infilled frames under seismic loads. For this purpose, six specimens represented by two-storey, one-bay brick infilled frames were tested under reversed cyclic loading. Furthermore, six infill panels were tested to determine the infill characteristics. Effects of plaster and concrete quality on infilled frames behavior were the main parameters investigated. The behavior of the infilled frames was compared with the behavior of bare frames. Analytical works was done to understand the stiffness, strength and behavior of these types of frames. From their experimental results they believed that the used hollow clay tile infill increases both strength and stiffness significantly for strength increases as compared to bare frame is about 240% in case the infill is unplastered and 300% for the plastered infill specimens from that it is clear to know that the plastering both sides of the infill improves the behavior. Comparing plastered and unplastered specimens, the strength increase due to the plaster is about 25% and increase in initial stiffness is about 50 to 80% and also the plaster delays the diagonal cracking of the infill. Plastered infill, cracks at about 20% higher load as compared to the unplastered specimen.

Mostafaei and Kabeyasawa (2004). They studied the presence of masonry infill walls and their responses under earthquake effect getting the results and compare it with the damage that occurred on the Bam telephone center is located about 1.5 km northeast of the 2003 Bam earthquake strong motion station. Their attempts were made to employ a realistic approach to modeling the infill masonry walls in the analysis of the Bam telephone center structure. The building was modeled for 3

different categories. First, in the category of BF, Bare Frame, the 3D bare frame of the building without stiffness and strength contributions of the infill walls are considered. However, infill wall masses on each floor are added to the mass of the corresponding floor. Second, in the category of FIM, Frame and Infill Masonry, the 3D structure is modeled considering the effects of strength and stiffness of infill masonry panels, as well as their masses. Finally, in the category of FIL, Frame and Infill Light panel. From their study they found a significant effect of infill walls on the structural response of the building and they obtain an analytical explanation of the almost linear performance of the building during the earthquake. It could be concluded that the Bam telephone center building without masonry infill walls would suffer large nonlinear deformations and damage during the earthquake. The maximum overall storey drift ratio of 0.8% was obtained for the ground floor of the building, which is less than a limit yielding drift ratio of 1.0%.

Calvi, Bolognini and Penna (2004). They presented a study observed the seismic performance of masonry infilled RC frames. In their experimental tests they investigated specimens represented by single-bay, single-storey 4.5x3 (height) m. They used equivalent diagonal strut for modeling the infill panel in their numerical analysis. Experimental and numerical results show in their study that frames with insertion and presence a little reinforcement in masonry infills and another specimens with unreinforced masonry panel comparing it with bare frame, from the results found that the slightly reinforced infill panel behavior gives significantly improved and be better than both unreinforced masonry infill and bare frame but particularly for what concern damage limit states the effects less important for a first cracking and a full collapse limit states.

To indicate the effect of the masonry infill walls on behavior of structure, a five storey reinforced masonry infill and bare frame building models ware selected and designed according to IS 1893 codal provisions. In building the infill walls are modeled by equivalent strut approach and the bottom storey of the building kept openly for considering the realistic behavior of the presently existing buildings in India. Nonlinear static and nonlinear dynamic analysis were performed to study the response behavior of the buildings. Three strong motion records from Imperial

Valley (1979), Northridge (1994) and San Fernando (1971) earthquakes are used to perform nonlinear analysis. Results shown that presence of infill walls greatly contribute the stiffness to lateral loads and the storey response quantities (displacement, storey shear) are decreasing due to the infill masonry walls. The location of plastic hinges concentrated at bottom stories causes sever structural damage in infilled frame structure at first storey but in the case of bare frame model hinges spread throughout the height of column. Srinivas and Prasad (2005).

Karayannis, Kakaletsis and Favvata (2005). In their study an analytical investigation and experimental observation of the influence of infill panels on the seismic behavior of reinforced concrete frames is presented. The project includes three 1/3-scale, single-storey, single-bay reinforced concrete frame specimens subjected to cyclic loading; one infilled frame specimen with clay brick solid masonry and two bare frame. For the contribution of the behavior of the infill to the response of the frame the equivalent diagonal strut model is used. Two different types of elements were employed for this purpose. The first element is an inelastic truss element with bilinear brittle response. The second one is an inelastic element with response that can include degrading branch and by using the element with degrading branch for the equivalent strut model yielded the most satisfactory results. From their experimental and analytical results we get that the influence of infill panel on seismic load is significant and increase the initial elastic stiffness and the lateral maximum capacity of the RC frames. From observing of the behavior of the specimens noticed that the main failure mode of the infill panel was in the form of diagonal cracking.

A typical six storey high apartment typed building with masonry infill wall with open soft first storey was considered in study done by Tuladhar and Kusunoki (2006). The main aim of this study was to investigate the seismic performance and design of the masonry infill Reinforced Concrete (R/C) frame buildings with the soft first storey under a strong ground motion. The study also highlighted the error involved in modeling of the infill RC frame building as completely bare frame neglecting stiffness and strength of the masonry infill wall in the upper floors. Rom this study noticed that the effect of infill wall changes the behavior of the structure

and it is important to consider infill walls for seismic evaluation of the structure and the Arrangement of infill wall in the frame affects the behavior of the structure.

Korkmaz, Demir and Sivri (2007) provide us with study of a 3-storey RC frame structure with different amount of masonry infill walls is considered to investigate the affect of infill walls on earthquake response of these types of structures. The diagonal strut approach is adopted for modeling masonry infill walls. Pushover is considered here as the load and the numerical analysis is obtained by using nonlinear analyses option of commercial software SAP2000. In this study the infill wall under investigation via nonlinear analysis and from the analysis results, it is noticed that the infill panels have a great effective on structure behavior under earthquake effect moreover, displacements exceed the limit level.

The effect of the Wechuan Earthquake, with a moment magnitude of 7.9 occurred in Sichuan Province in China on May 12, 2008 is investigated by Kermani, Goldsworthy and Gad (2008). This study focuses specifically on observations made on this type of construction during the visit to Sichuan with identification of damage and of key failure modes. This will be related to the damage and failure modes observed in past earthquakes and in experimental work. From their observation for the damage that happened in the building that effected by the earthquake they reported a various types of damage and failure modes, which happened in the infilles panels and RC frames in the remaining buildings. It was observed that in some cases the structural interaction between the frame and infill improved the seismic behavior relative to the frames acting alone. The modes of failure observed in different infill-frames were similar to those observed by researchers in their experimental studies.

Taher and Afefy (2008) presented in their study a comparing between nonlinear analysis for RC frame with masonry infill panel modeled by original system and infill panel modeled by unilateral diagonal struts for each bay only activated in compression. The influence of partial masonry infilling on the seismic lateral behavior of low, medium, and high-rise buildings is also addressed. The most simple equivalent frame system with reduced degrees of freedom is proposed for handling multi-storey multi-bay infilled frames. The suggested system allows for nonlinear finite element static and dynamic analysis of sophisticated infilled reinforced

concrete frames. The effect of the number of stories, number of bays, infill proportioning, and infill locations are investigated. Geometric and material nonlinearity of both infill panel and reinforced concrete frame are considered in the nonlinear finite element analysis. The results of this study reflect the significance of infill in increasing the strength, stiffness, and frequency of the entire system depending on the position and amount of infilling. Moreover the nonlinear finite elements, which represented by with unilateral diagonal strut yields reasonable predictions with the results of the original system.

An experimental study of a full-scale three-storey flat-plate structure strengthened with infill brick walls and tested under displacement reversals was done in Purdue University by Pujol, Climent, Rodriguez, and Pardo (2008). The results of this test were compared with results from a previous experiment in which the same building was tested without infill walls. The addition of infill walls helped to prevent slab collapse and increased the stiffness and strength of the structure whereas the structure with no infill experienced a punching shear failure at a slab-column connection. A numerical model of the test structure was considered and compared with experimental results. The measured drift capacity of the repaired structure was 1.5 % of the height of the structure. These additional walls were effective in increasing the strength (by 100%) and stiffness (by 500%) of the original reinforced concrete structure.

A study was taken the influence of brick masonry panels on cyclic response of RC frames, a bare frame and several infill frames were tested by Cesar, Oliveira and Barros (2008). The numerical analysis results that based on the nonlinear analysis and inelastic hinge method either for bare frame and the infill frame using commercial FEM package are compared with the experimental results that got from the done tests. The numerical results show that is possible to get accurate results and so close with the results that got from experimental results, if a correct computational model is selected. The observed behavior from experimental test is more detailed from the one that got from the numerical analysis. The evaluation showed that the brick masonry infilled frame behavior is improved greatly when comparing it with bare frame.

Kermani, Goldsworthy and Gad (2008). The predictions of FE models for masonry infill RC frames under seismic load were compared with the results of some laboratory tests that were conducted at the University of Melbourne on masonry specimens. The aim of this research is the better understanding of the interaction between the RC frame and masonry infill wall and understanding the behavior of such a structure under earthquakes. The modeling techniques, which developed by using ANSYS in this research, will be useful to evaluate the real performance of infill frames when subjected simultaneously to seismic load.

Vaseva (2009) presented in his study the effect of the masonry infill wall on the RC frame and observing the relationship between the infill wall and the boundary frame. Both micro (panel element) and macro (strut element) models were considered for modeling the infill panels. The results from nonlinear analysis of the bare and infilled frames are compared. From the results of this study it is shown that with the application of the strut model it is possible to give good solution for infill frame evaluation and the presence of masonry infill walls can affect the seismic behavior of framed building. These effects are generally positive: masonry infill walls can increase global stiffness and strength of the structure. The energy dissipation capacity of the frames with infill walls is higher than that of the bare frame.

Sattar and Liel (2009) present a study assesses the seismic performance of building represented by masonry infilled RC frames, utilizing dynamic analysis of nonlinear simulation models to obtain predictions of the risk of structural collapse. The evaluation is based on structures with design and detailing characteristics representative of California construction. In this study different specimens are investigated considered by bare, partially-infilled and fully-infilled frames, the fully-infilled frame has the lowest collapse risk and the bare frame is found to be the most effected specimen to earthquake. The presence of masonry infill also significantly changes the collapse mechanism of the frame structure. The better collapse performance of fully-infilled frames is associated with the larger strength and energy dissipation of the system, associated with the added walls. Similar trends are observed for both the 4 and 8 storey RC frames.

Recognizing that many of the previously studies on this subjects have been used equivalent diagonal strut to model the infill panel and from the results all researchers believe that the masonry infill walls have the significant effect on the structures behavior under seismic load. Infill proportioning, and infill locations are also investigated in some studies. The results we got reflect the significance of infill in increasing the strength, stiffness of the entire system depending on the position and amount of infilling so should not ignore the effect of infilles and should take a full consideration at structures design.

1.3 Research Objectives

Structural engineers, during the design process of a building, typically, ignore the effects of infill masonry walls in the structural analysis. The only contributions of masonry infill walls are their masses as non-structural elements. Consequently, analyses of the structures are based on the bare frames. In the last 4 decades, the effects of infill walls in frame structures have been extensively studied. Experimental and analytical study results show that infill walls have a significant effect on both the stiffness and the strength of structures. Studies have also been done to obtain analytical models that consider the effects of infill walls in the analysis. Therefore, in the present study, it is estimated that the infill masonry walls might have major effects on the building performance, leading the structure to perform almost linearly.

Three specimens have been done in Dokuz Eylul University, structure mechanics laboratory, one of them is bare frame and different type of clay bricks is considered as infill for the two others. The specimens were in half scale with 137.5 cm height and 200 cm width, single bay and single storey. The main characteristics of the specimens were 200 kg/cm^2 and the profile of the reinforcements steel was 6∅8 for the columns and 4∅8 for the beam. The bare frame is used as a control specimen to understand the effect of two different kinds of clay bricks. In other hand the analytical study was implemented by using OpenSees and after modeling the specimens and understand the effect and the behavior of infill panel represented in

two different types of clay bricks, the effect of number of bay and soft storey is studied.

CHAPTER TWO

CORROBORATION STUDY OF RC FRAME WITH MASONRY INFILL

2.1 Infill Panel and Frame Structures

Infill panel is a campsite materials contain generally from masonry unites like clay bricks or concrete blocks, which could be supported by reinforcement or not and mortar beds all covered by plastered. Reinforced and unreinforced concrete panels are also used depends on purpose. The reasons for using masonry as infill materials widely in concrete structures are; (1) Cheaper materials with low cost labour availability make this material the preferred choice for under developed or developing countries and it has good strength against bad weathers. (2) The people feel much more secure if the environment that they are living in are built using solid walls. It is very important to have solid walls for the majority of people from different cultures.

Reinforced concrete (RC) frames consist of horizontal elements (beams) and vertical elements (columns) connected by rigid joints. Although the RC frames structures are widely used as a structural system but most of the time and throughout the previous decades the infill panel is considered as a non-structural elements as a non-structural elements and it was just considered as a weight in design and ignore its effect but after a lot of studied done by many researchers noticed the significant effect especially on seismic load. The reasons that made some researchers to not take the infill panel in consideration at first; (1) The complexity that is found at calculating the rigidity of infill panel; (2) There are not a lot of documents provide them with studies investigating totally the behavior of infill panels in the design.

Recently there are many studies are done by different researchers try to understand the real behavior of infill panels and consider it as structural element.

2.2 The Roll of The Masonry Infill Panel Under Earthquake

The masonry infill changes the mass, damping, stiffness and strength properties of the whole integrated structure. Many studies acknowledge the difference between a bare frame and an infill-frame. However it is important to realize the roll that the infill panel has on structures behavior.

During an earthquake, these infill walls will increase the lateral earthquake load resistance significantly and often will be damaged prematurely, developing diagonal tension and compression failures. The degree of lateral load resistance depends on the amount of masonry infill walls used. However, for the reasons explained above, masonry infills are commonly used in internal partitioning and external enclosure of buildings, increasing wall-to-floor area ratios. Therefore, in spite of the lower strength and expected brittleness of this type of masonry walls, the frames benefit from the extensive use of masonry walls until the threshold of elastic behavior has been exceeded.

Beyond the premature failure of brittle masonry, the sudden loss of significant stiffness against lateral drift must be compensated by the slab/beam-column junction of the frame structure. This behavior causes a high drift demand on the frame members, hence causing increased damage to the structure if there were no masonry infills.

The sudden loss of stiffness in the lateral load resistance mechanism causes a very high concentration of loading. This increased magnitude of loading causes significant damage or even the collapse of slab/beam-column joints. If one or two joints collapse others will follow.

2.3 Failure Modes of Infilled Frames Structures Under Seismic Load

The earthquake have revealed several patterns of damages and failure in masonry infilled RC frame constructions. At low levels of cyclic forces, the frame and the infill panel will act in a fully composite fashion, as s structural wall with boundary

element. As lateral deformations increases, the behavior becomes more complex and the result is separation between frame and panel at the corners on the tension diagonal, and the compression diagonal represented by diagonal compression strut.

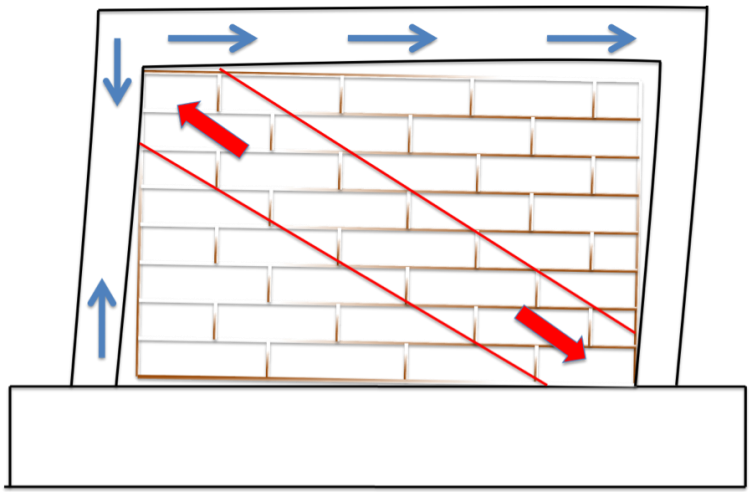

Figure 2.1 The separation between the surrounding frame and infill panel causes the compression strut.

At the time of separation of the infill panel cracks occur on the plastered that cover the infill panel from outside. At the first the cracks are small getting bigger by increasing the lateral load. The cracks starts at beam-infill panel and column-infill panel contact areas.

According to the masonry infill wall, there are several different possible failure modes like sliding shear failure along the horizontal mortar, it happens generally at or close to mid-height of the panel. Compression failure of the diagonal strut, for typical masonry infill panels crushing happens at corners that suffered from compression load. the compression failure consider as the final panel failure mode thus the compression strength that occur the failure may used as the ultimate capacity for the panel.

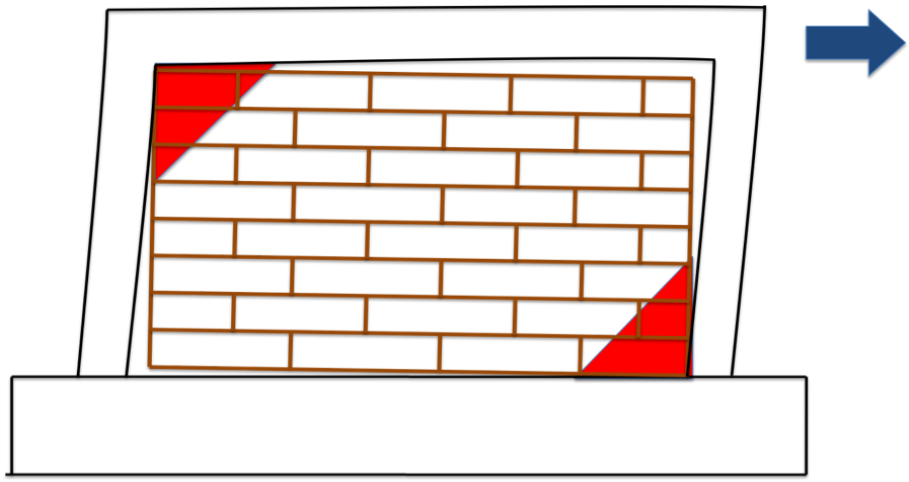

Figure 2.2 Compression strength causes crushing the corners.

According to the RC frame there are a lot of failure mode for RC frames like; shear failure and concrete crushing failure in concrete columns. There are the most undesirable non-ductile modes of failure

Figure 2.3 Shear failure of a reinforced concrete column (EERI 2001).

Flexural plastic mechanism represented by Plastic hinges at member ends and Plastic hinges at span length occur after failure modes that occur on masonry infill panel and also Failure due to axial loads like Yielding of the reinforcement.

Inappropriate column/beam relative strengths. This can lead to failure of individual members and connections when the “weak column-strong beam” mechanism developes.

2.4 Discussion of Modeling The Masonry Infilled RC Frames

Fiber section method is used to model the RC concrete frame. The fiber model is a methodology that can be used to model and analyze nonlinear behavior of the RC frame and is based on the discreization of a section in elements or fibers that associated to each material with axial deformation.

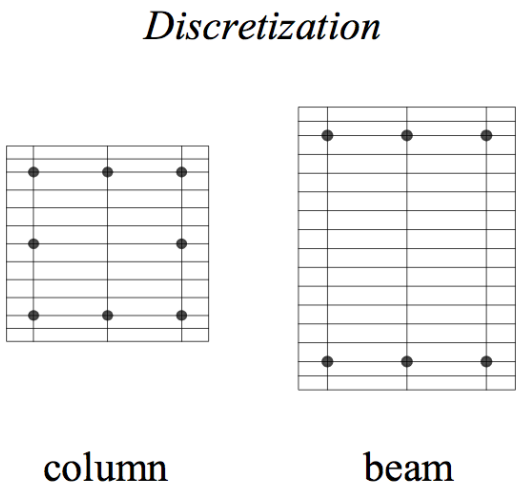

Figure 2.4 Discretuzation of beam and column.

This methodology presents a good approach to experimental model and it consider as one of successful modeling method of RC frames.

The analytical modeling of infilled frames is a complex issue, because these structures exhibit highly nonlinear inelastic behavior, resulting from the interaction

of the masonry infill panel and the surrounding frame. The masonry infill wall is modeled using either equivalent strut model or a refined continuum model.

In this research Equivalent diagonal strut is used to simulate the masonry infill panel as represented in Figure 2.5.

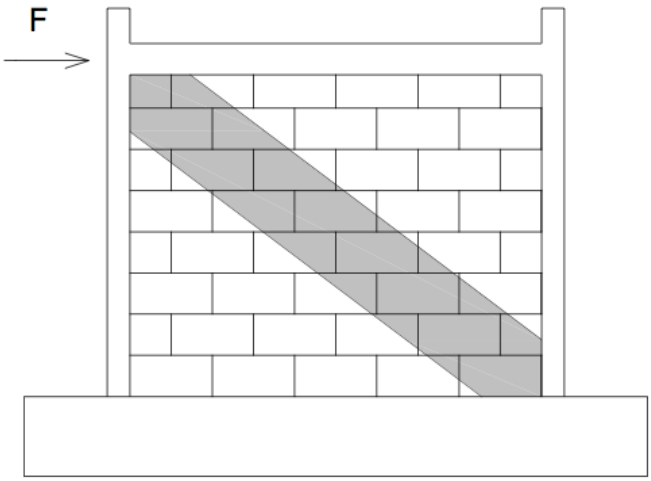

Figure 2.5 Equivalent diagonal strut.

There are some limitations about using compression strut by ignoring the interactions between the infill panel and the surrounding frame and it is also not possible to be predicted the damaged area of masonry either. Using diagonal struts is not straightforward, especially when there exist some openings, such as doors or windows, in the wall. But most of the researchers have used the diagonal strut to simulate the infill panel because it gives good results and so close to the experimental results by calculating the geometry of the strut carefully. To simulate the masonry infilled RC frame under seismic load in this research OpenSees analysis program is used.

2.5 United States Procedures

2.5.1 FEMA

The NEHRP Guidelines for the seismic rehabilitation of buildings (FEMA) is an extensive document for use in the design and analysis of seismic rehabilitation projects. FEMA-273 includes design criteria, analysis methods, and material specific evaluation procedures. Section 7.5 addresses masonry infills systems.

FEMA publications on the Evaluation of Earthquake damaged concrete and masonry wall buildings (FEMA-306 1999, FEMA-307 1999) were developed to provide practical criteria and guidance. FEMA-306 recommends that infill panels may be modeled as equivalent struts in accordance with FEMA-273. Deformation capacity guidelines are given in the form of interstorey drift ratios. These vary from 1.5% for brick masonry to 2.5% for ungrouted concrete block masonry. As diagonal cracking is initiated at drifts of 0.25% and essentially complete by about 0.5% this represents a high level of ductility in the panel system.

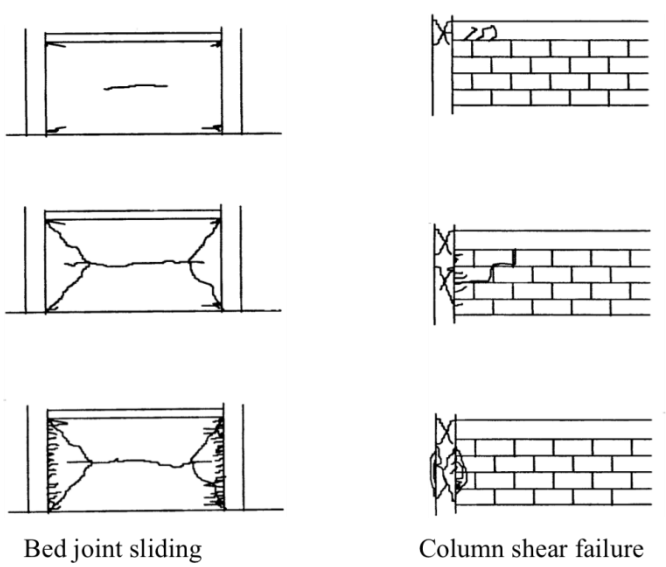

Figure 2.6 Component Damage (FEMA-306 1999).

For the concrete-frame components, shear demand is evaluated for short columns as specified in FEMA-273. FEMA-306 also provides an infilled frame component

damage guide. Two topical behaviour modes are illustrated in Figure 2.6. The bed joint sliding mode involves diagonal cracks from the corners intersecting horizontal cracks in centre of the panel and is associated with large displacements as may be found with flexible steel frame. The reinforced concrete column shear failure mode typically occurs near the frame joints and is associated with stiff and/or strong infills.

2.6 European Procedures

2.6.1 Eurocode8

Eurocode 8 (EC8) [DD ENV 1998-1 1996] contains provisions for the design of infilled RC frames (section 2.9). EC8 specifies that the period of the structure used to evaluate seismic base shear shall be the average of that for the bare frame and the elastic infilled frame. Frame member actions are then determined by modeling the frame with the struts. Irregular infill arrangement in plan and elevation are addressed.

2.7 OpenSees

In our research OpenSees is the program that we will use to modeling the RC frame with masonry infill wall under seismic load. OpenSees is integral to achieving the PEER Center's goal of advancing performance-based earthquake engineering. OpenSees is "a software framework for the nonlinear finite element modeling and analysis of the seismic response of structural and geotechnical systems" (http://opensees.berkeley.edu). It serves as the primary computational platform for PEER sponsored research geared toward advancing performance based earthquake engineering. Previous studies by other researchers resulted with the development of modeling the equivalent diagonal strut RC frames and constitutive models that have been implemented in the OpenSees platform and made available for use by the earthquake engineering research community.

This research takes advantage of the newly available modeling tools in OpenSees to simulate RC frames with masonry infill wall under seismic load. The sub-assemblage is the result of experimental works completed at the University of California (Mostafaei and Kabeyasawa 2004 and Hashemi and Mosalam 2007), they used OpenSees to modeling the RC frame with masonry infill in many studies as following:

Concrete is modeled using uniaxial stress-strain relationships. Cover and core concrete materials were defined separately implementing the model and referred to as Concrete01 in OpenSees. Steel reinforcement is modeled and referred to as Steel01 in OpenSees. Whereas concrete01 in OpenSees compression only is used to model the equivalent diagonal strut representing the infill wall.

The following free body diagram will be helpful to understand how to handle any problem modeling and analysis it with OpenSees. The processes of OpenSees are in two main steps domain and analysis as showing in Figure 2.6.

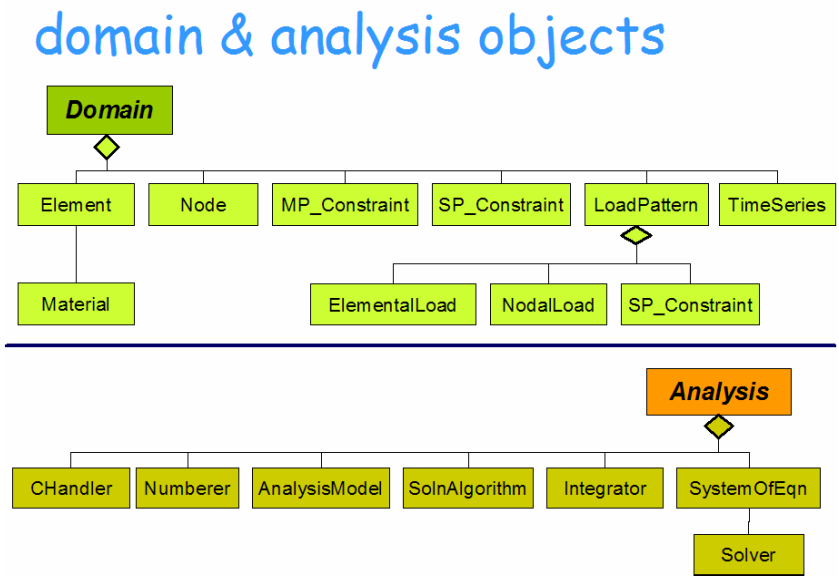

Figure 2.6 OpenSees processes objects.

CHAPTER THREE

EXPERIMENTAL WORK

3.1 Introduction

In this chapter will be discussed three experimental works have been done in Dokuz Eylul University, Civil engineering department, structure mechanics laboratory on three specimens RC frames single bay-single storey one of them was bar frame and the two others were infilled with different types of clay bricks, first type is standard brick being used in Turkey and second type is called locked brick, both of them are clay hollow bricks with different parameters as see Table 3.2, and Figure 3.1 is showing the dimensions for each of a) locked and b) standard. The main purpose of testing three specimens bare frame and two infilled panel frames with different characteristics to be able to compare between them and understand the effect of the infill panel under seismic load and how much the structure is effected by changing the characteristics of the clay bricks.

In these tests half- scale RC frames were taken into consideration with dimensions as shown below in Table 3.1. To get realistic results, clay bricks were also used with half-scale to give the realistic behavior inside the infill panel as shown in Table 3.2.

Table 3.1 Dimension of the half-scale RC frame.

Element	Width (mm)	Depth (mm)	Length (mm)
Beam	150	250	Between columns center lines 2000
Column	150	250	From connection point with the foundation to beam center line 1375

Table 3.2 The properties of clay bricks that used in experimental works with half-scale.

Brick	Length (mm)	Width (mm)	Height (mm)	Void Ratio %
Locked	125	110	75	40
Standard	125	110	60	34

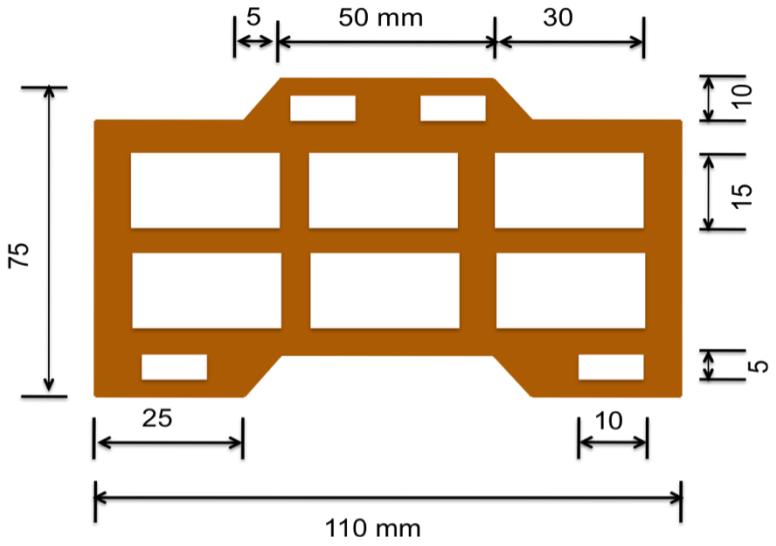

a) Locked brick.

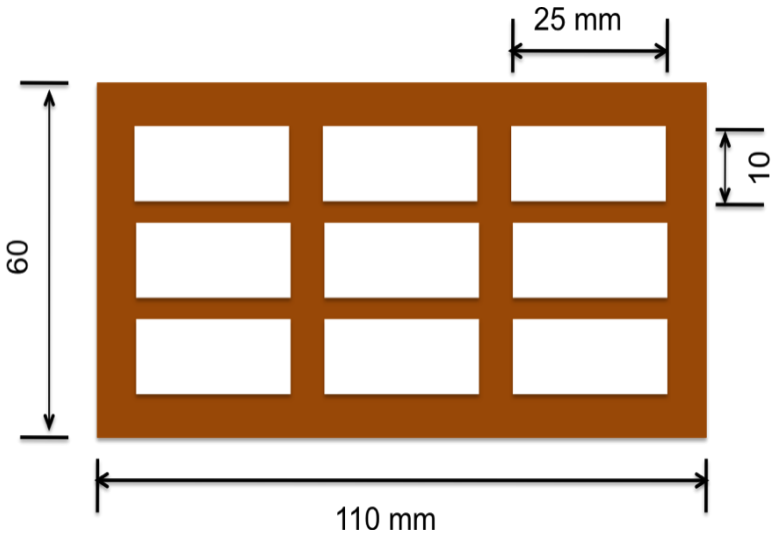

b) Standard brick.

Figure 3.1 The dimensions for each of locked and standard bricks.

3.2 Design of Half-Scale Test Frame

The loading and design of the test frame is meant to be as realistic as possible to ensure that the experiment produces meaningful data that can be applied to real world structures. This achievement of realism must also be balanced with laboratory limitations and constraints, some of which include the available lab space, actuator capacities, and funding. The dimensions of the half-scaled RC frame informed previously in Table 3.1. In addition to this, some of the important design parameters and their impact of the behavior of the frame like reinforcement bars, bars in columns are 6∅8 in beam 4∅8. The foundation is built with dimensions 3000 mm, 550 mm and 500 mm length, width and height, respectively.

3.3 Test Setup

Test setup is the first step at any experimental work. The testing works of the three specimens have done in Dokuz Eylul University, Civil engineering department, structure mechanics laboratory, where all the facilities were available that the testing works of RC frame under seismic load need. Placing the specimen and montage it tightly to prevent the horizontal and rotation movement of the foundation and to not get big error in the values in the top displacements that we will be taken later and placing it near to compressor at top column-beam joint. After placing the specimen, the infill wall are built, if the test is considered with infill wall if is not, next step is run.

Divide the frame to cells by drawings lines after coloring it with appropriate color like white and the lines with black color to record the exact location of the damage during the test as shown in Figure 3.2.

Before connect the compressor to frame, the compressor should be calibrated well to get the right load results that will be recorded from the compressor. Connect the head of the compressor with a plate at top column-beam joint and install two bars connecting two plates one of the plate at the head of the compressor and the other is placed at the other top column-beam joint to provide the pushing and the pulling that are happening in the cyclic load. Placing the sensors at different locations as it is

shown in Figure 3.3 to record all the changes observed in displacements and strain gauges to record the strain at steel bars, from 1st to 13th sensors measure the displacements and from 14th to 25th the sensors measured the steel bars strain during the test. After placing the sensors and checking their levels, record and conform the initial value of the sensors. After doing all the processes that were discussed above the specimen is ready to be tested (see Figure 3.4).

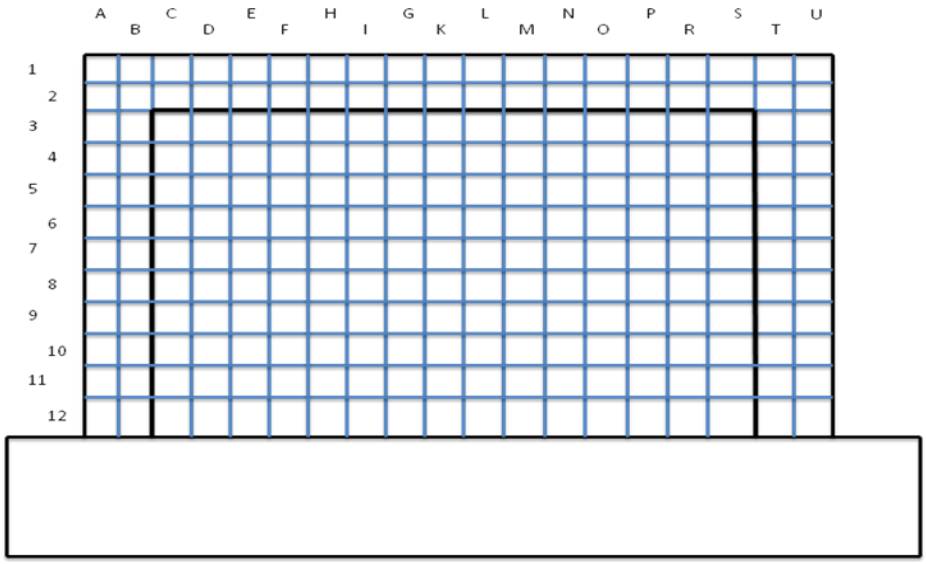

Figure 3.2 Dividing the Frame to confirm the exactly damage location during the test.

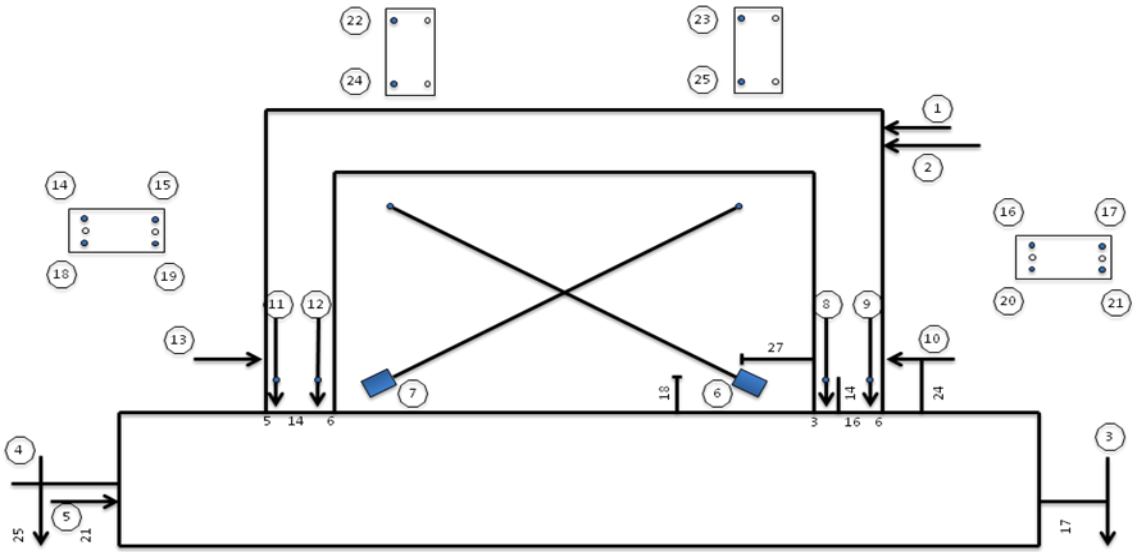

Figure 3.3 Displacement and steel bar sensors locations on frame.

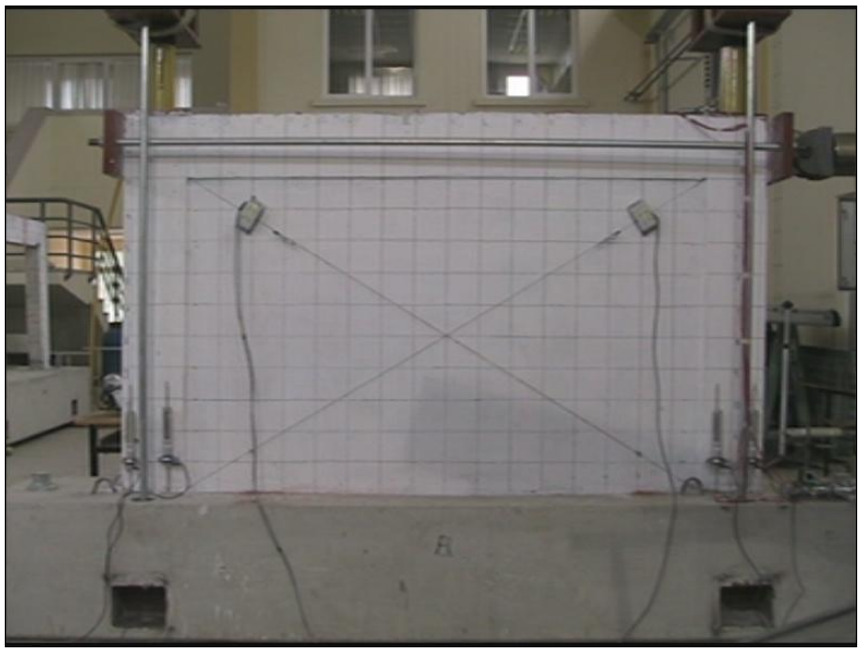

Figure 3.4 Experimental Specimen of Masonry Infilled RC Frame Tested in Dokuz Eylul University.

3.4 Loading Protocol

Extensive nonlinear static and dynamic time-history analyses were performed using the analysis program OpenSees (McKenna et al. 1999) prior to testing. According to test we can define the load protocol in two steps, first we will apply a gravity load as an axial force represent the load that would come from above storey pointed at top of the column-beam joints at two points with 10 Tons. Applied loads were recorded from manometer. The lateral load, which would be applied from the compressor at the one of the column-beam joints to get the aim displacement at each cycle, is considered as the second load protocol.

3.5 First Test: Bare frame

In the first test, half-scale bare frame was tested under seismic load. Bare frame was setup in the Dokuz Eylul University, Civil engineering department, structure mechanics laboratory to be investigated all the damages that would happen under earthquake effect by applying cyclic load. The purpose from investigating the bare frame is being able to compare the results with infilled frame and understand the effects level of the masonry infill with different kinds of clay bricks. At the first test the drift ratio was implemented at 54 cycles with Increment at every three cycles to obtain load degradation at each cycle. The applied drift at the frame is shown in the Figure 3.5.

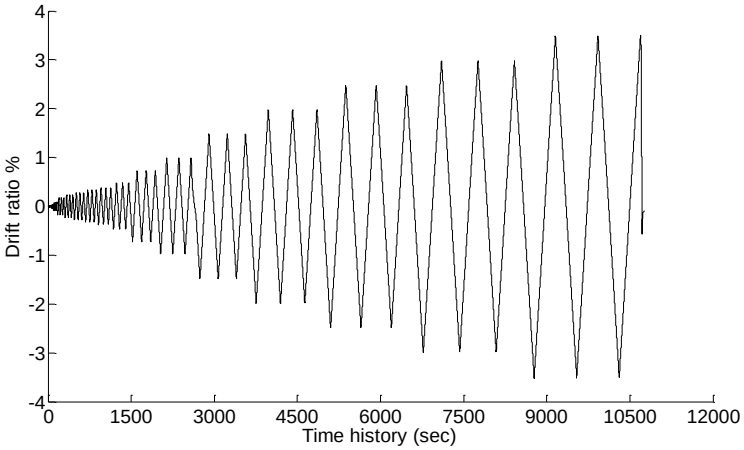

Figure 3.5 Drift ratio and time history under applied quasi-static load at second test infilled RC frame.

By giving the start to get the aim displacement at each cycle, consequently a lateral load are being applied to give the displacement that we aim to. By applying displacement pattern increasing at every three cycles, load degradation is being the Resultant of this repeating as shown in the load curve of the bare frame in Figure 3.6.

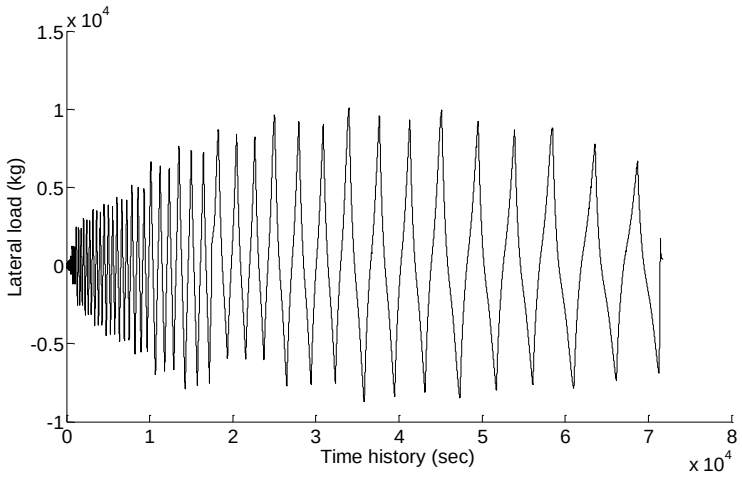

Figure 3.6 The lateral load and time history in first test (bare frame).

Single storey- single bay under cyclic load bare frame with maximum drift ratio 3.5%, with approximately maximum load of 10 Tons. The hysteretic response for bare frame under cyclic load shown in Figure 3.7.

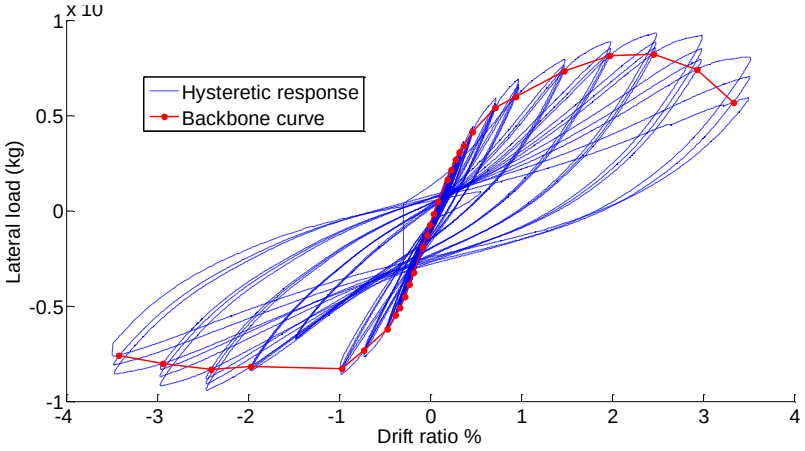

Figure 3.7 Hysteretic response of the bare frame under cyclic load (experimental results).

3.6 First Test Results

The bare frame test was conducted in 2010. Testing was recorded via live video including real-time data plots. The response of the frame was monitored and documented with over 20 channels, visual inspections, and photographic images. Instrumentation was set up to measure the rotations in the RC frame elements and the occurring lateral movement and rotation in the foundation and the strains in the reinforcement bars in the columns and the beam. Table 3.3 below shows the type of failure, the value of the displacement, the load the cyclic and the position for each failure mode.

Table 3.3 The damage progress during the first test.

No.	Damage Type	Cyclic No.	Drift % for actual position	Actual Disp. (mm)	Load at actual position	Cyclic Max. Disp. (mm)	Cyclic Max. Load (kg)	Cell nu.
1	Column Bottom	57	0.155	2.137	983	3.842	2742	U11
2	Column bottom flexure	63	0.212	2.917	1583	4.41	3106	U10
3	Column Beam connection corner	72	0.008	0.11	-1062	4.639	-5087	B2
4	Column top flexure	73	0.226	3.11	1684	5.097	3074	T3
5	Column Beam connection Point	77	0.227	3.115	1545	5.077	3435	A2
6	Column bottom flexure	81	-0.3	-4.13	-4200	-6.636	-6256	U11
7	Column flexure	86	-0.52	-7.15	-6512	-10.05	-7680	A4
8	Column beam connection shear	89	0.282	3.881	1397	9.901	5498	B2
9	Column top crack	91	0.574	7.89	3997	13.38	6906	U3
10	Column Foundation separation	93	0.647	8.89	4032	13.38	6619	U12
11	Column bottom shear	94	-0.98	-13.48	-8375	-13.48	-8375	A12
12	Beam Flexure	96	-0.573	-7.88	-5323	-13.56	-8263	S1
13	Column Beam separation	99	1.48	20.35	7653	20.35	7653	U3
14	Column bottom crushing	100	-1.481	-20.36	-6729	-20.36	-6729	U12
15	Column bottom	101	1.479	20.34	7490	20.34	7490	A12
16	Cover concrete failure	102	-1.481	-20.36	-6721	-20.36	-6721	S2
17	Crack 3 mm	109	2.488	34.21	9343	34.21	9343	U12
18	Beam bottom	110	-1.445	-19.87	-6473	-33.88	-9425	C2
19	Column bottom steel bar buckling	122	-1.956	-26.89	-6121	-47.82	-8495	U12
20	Steel bar failed	128	1.591	21.88	2687	48.88	5903	U12

and Figure 3.8 represent the hysteretic response for the bare frame and all the failure types that mentioned in Table 3.3 is located on figure.

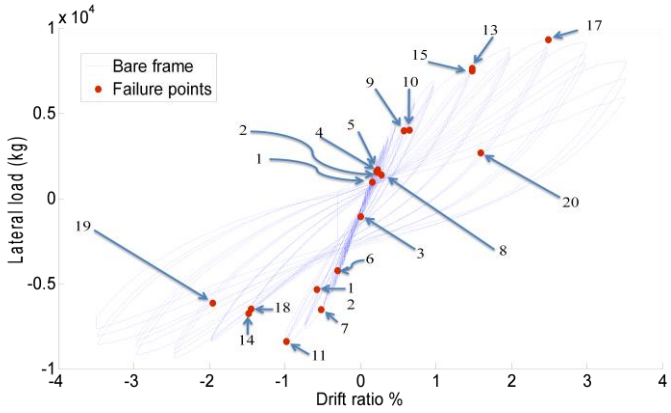

Figure 3.8 Drift ratio and lateral load values for each failure point.

3.7 Second Test

Standard Brick infilled frame is the second test that was done in 2010 in Dokuz Eylul University, Civil engineering department, structure mechanics laboratory. In this test standard brick was used as the infill with half-scale to get more realistic results because the single storey-single bay RC frame was also with half-scale. In the test the behavior and effect of the infill panel were being investigated. In this test 54 Cycles have done Increment occurring at every three cycles. The maximum drift ratio is in the last cycle with value 3.5% of the height of the column 1375 mm, Figure 3.9 showing the drift ratio that implemented in second test. The mortar layer between the brick is used just horizontally.

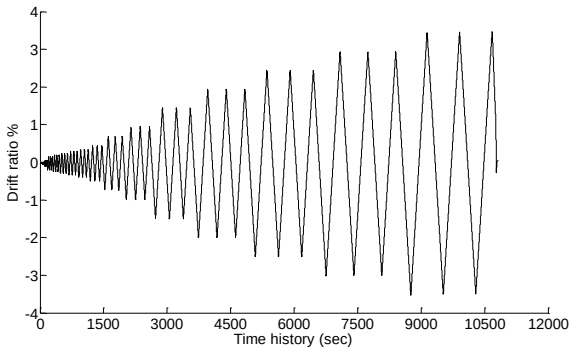

Figure 3.9 Drift ratio v.s. time history under quasi-statically applied load during the second test (infilled RC frame).

To get the displacement that we are looking forward to a lateral load is being applied from the compressor with different values according to displacment ratio, Figure 3.10 showing the lateral load curve according to the second test.

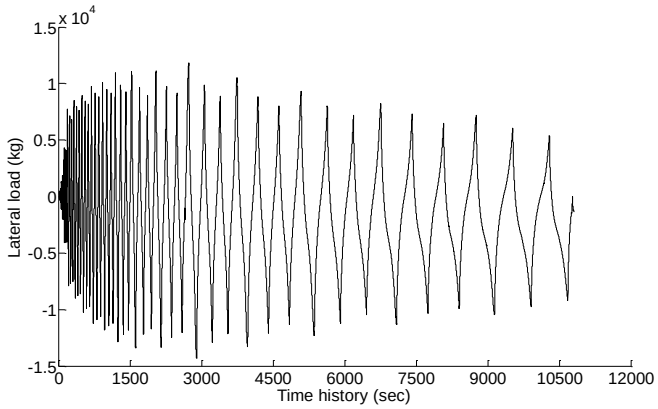

Figure 3.10 The lateral load applied during second test (infill frame with standard bricks).

Single storey- Single bay under cyclic load standard brick infilled RC frame maximum drift ratio 3.5%, with approximately maximum load 13.800 ton. Frame's drift and lateral load relationship shown in Figure 3.11.

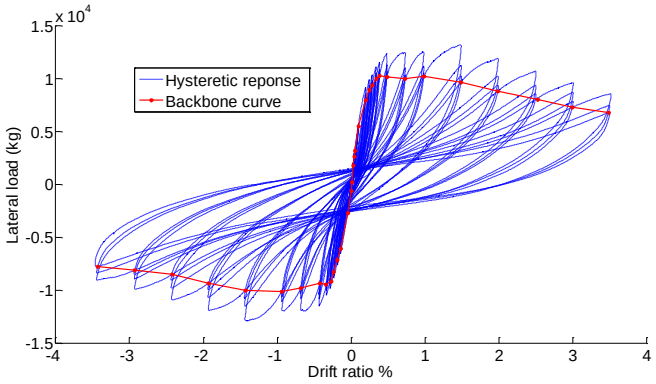

Figure 3.11 Hysteretic response of the standard brick infilled frame under cyclic load (experimental work).

.

3.8 Second Test Results

A cyclic load was performed in the standard brick infilled RC frame test. The same preparing that has been done at first test by giving attention to infill panel by putting displacement measurement to understand the behavior of the infill wall

before the failure. The first noticed failure was recorded at the drift ratio 0.1372% with displacement 1.8865mm beam wall separation and Table 3.4 showing drift ratio and lateral load values for each recorded failure and giving the failure position at Hysteretic response of second testing Figure 3.12**.**

Table 3.4 The damage progress during the second test.

No.	**Damage Type**	**Nu. Of Cyclic**	**Drift % for actual position**	**Actual Disp. (mm)**	**Load at actual position**	**Cyclic Max. Disp. (mm)**	**Cyclic Max. Load (kg)**	**Cell nu.**
1	Beam Panel Separation	51	0.1372	1.8865	4842	3.435	9847	KO-3
2	Left Column Panel Separation	51	0.0082	0.112	-154.9	3.435	9847	C3-5
3	Plaster cracking	53	0.0809	1.112		4.68		
4	Column Top Cracking	63	0.0809	1.112	2196	4.68	11110	T3
5	Panel Foundation Separation	68	0.0082	0.11275	983.8	5.323	12000	CS-12
6	Flexure failure at column bottom	89	0.0645	0.886	1778	10.13	10920	A12
7	Beam Connection Point Failure	92	-0.1537	-2.113	-2355	-12.87	-11360	B2
8	Beam Flexure Failure	93	0.7918	10.88	8610	13.59	11730	D2
9	Flexural Failure	94	-0.5736	-7.887	-5574	-12.93	-10420	C2
10	Vertically Cracking	98	-0.8809	-12.112	-8560	-19.74	-12310	S 1-2
11	Failure at the Depth Side of the Beam	103	0.8082	11.112	4877	27.4	12480	P1
12	Crushing at Column Bottom	104	-1.0991	-15.1126	-6778	-26.58	-11320	U12
13	Brick breaking	106	-1.5355	-21.113	-7708	-26.63	-10050	PR-9
14	Bricking Breaking (Cross Separation)	109	1.0264	14.113	4714	34.47	11200	E6
15	Crack at the topside of the Beam	110	-1.1554	-15.886	-4985	-33.45	-10280	E1
16	Bricks Separation	111	1.7372	23.88	6552	34.47	9976	E8-9 F9 G9
17	Beam Column Connection Point plastic hinge	116	1.7537	24.113	5619	41.38	10210	S1
18	Increasing of depth of Cracking at Column Beam Depth	118	1.8264	25.113	5284	41.37	9299	S1-U3
19	Beam Column Connection	121	1.3009	17.887	3482	48.45	9151	BC-1
20	Reinforcement Buckling at The Bottom of the Right Column	121	-2.6991	-37.1126	-6836	-47.38	-8421	U12
21	Cover Concrete Crushing at the bottom side of The Beam	122	3.5	48.17	8003	48.17	8003	RS-2
22	Bricks Falling	123	-3.44	-47.4	-7716	-47.4	-7716	CDE-6

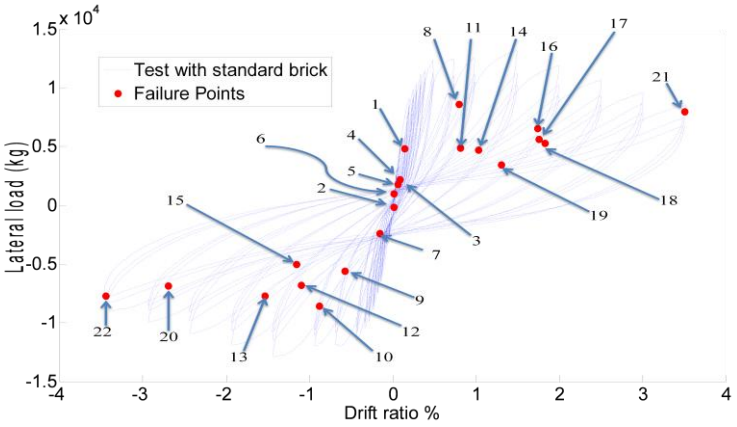

Figure 3.12 Drift ratio and lateral load values for each failure point.

3.9 Third Test

In Dokuz Eylul University, Civil Engineering Department, structural Mechanics Laboratory three tests were performed. The first test was a bare RC frame and the second one was RC Frame infilled with standard brick, in this section the third test is discusseded. The third test was infilled with clay brick called locked brick. Locked brick has different characteristics from standard brick. The main purpose from using the locked is being able to comapre the effect of the infill panel with different kind of bricks. In the test the behavior and effect of the infill panel were being investigated. In this test 50 cycles have done Increment occurring at every three cycles. The maximum displacement is in the last cyclic with drift ratio 2.5% of the height of the Column 1375 mm, Figure 3.13 show us the drift ratio that implemented in third test. In this test no mortar is used between the bricks just between the infill panel and the surrounding frame

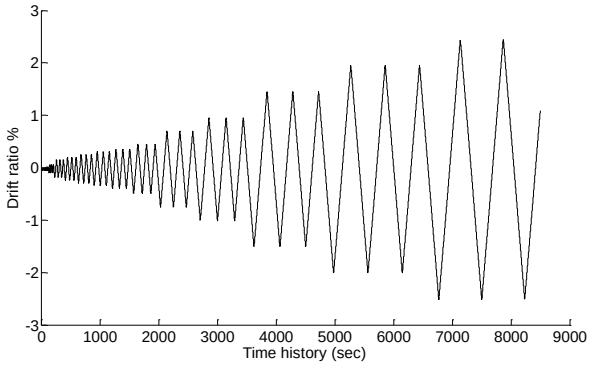

Figure 3.13 Drift ratio and time history at second test infilled RC frame.

To get the displacement that we are looking forward to a lateral load is being applied from the compressor with defferent values according to displacment ratio, Figure 3.14 showing the lateral load curve according to the third test.

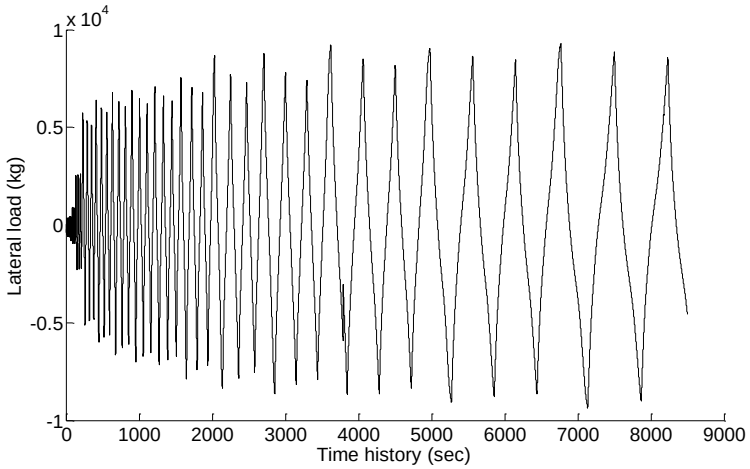

Figure 3.14 The larteral load that applaied in third test infill frame with Locked bricks.

Single storey- Single bay under cyclic load for the frame infilled with locked brick maximum drift ratio 3.5%, with approximately maximum load 10.0 tons. Frame's drift ratio and lateral load relationship shown in Figure 3.15.

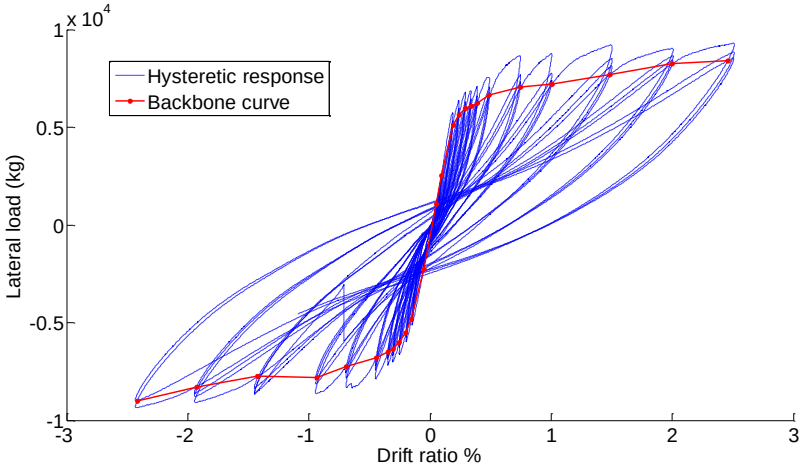

Figure 3.15 Hysteretic response of the locked brick infilled frame under cyclic load in experimental work.

3.10 Third Test Results

A cyclic load was performed in the locked infilled RC frame test. The same preparing that has been done at first and second test by giving attention to infill panel by putting displacement measurement to understand the behavior of the infill wall before the failure. The first noticed failure was reordered at the drift ratio -0.0574% with displacement 0.78925mm beam-wall separation and Table 3.5 showing displacement and lateral load values for each recorded failure.

Table 3.5 The damage progress during the third test.

No.	Damage Type	Cyclic No.	Drift % for actual position	Actual Disp. (mm)	Load at actual position	Cyclic Max. Disp. (mm)	Cyclic Max. Load (kg)	Cell nu.
1	Beam Panel separation	53	0.0574	0.789	1418	3.306	6347	I3
2	Column Panel Separation	56	-0.2217	3.048	-5508	3.494	-5918	C3-7
3	Plaster Cracking	57	0.08161	1.122	1751	4.023	6922	K6-N9
4	Flexure at column bottom	71	0.1489	2.047	2324	5.357	6969	B11
5	Column Beam Connection point failure	74	-0.2217	-3.0483	-3471	-6.188	-7278	B2
6	Flexure at column top	85	0.142	1.952	1937	10.13	9268	B10
7	Failure at Plaster Shell	87	0.6511	8.952	7273	10.3	8304	M6-O7
8	Beam Flexure Cracking	91	0.5056	6.952	4710	13.82	9381	C1
9	Column Foundation Separation	92	-0.2217	-3.0483	-2618	-12.99	-8033	B12
10	Flexure shear at Column Top	95	0.942	12.95	7490	13.87	8000	-
11	Column Beam Connection point Shear failure	96	1.5	20.62	9797	20.7	9797	T2
12	Cracking width 1.5 mm	103	0.5783	-.951	3149	27.62	9653	U12
13	Compression Crushing (Reaching the Crushing Deformation Unit)	108	-1.7126	-23.54	-8022	-26.62	-8022	C3
14	Cracking width 3.5 mm	115	-2.3238	-31.952	-8417	-33.47	-8417	U12
15	Start Occurring of Plastic Hinge at Column Bottom	116	2.5	34.37	9159	34.4	9159	-

It can also possible to observe the failure mode and give the position at Hysteretic response of third test from Figure 3.16**.**

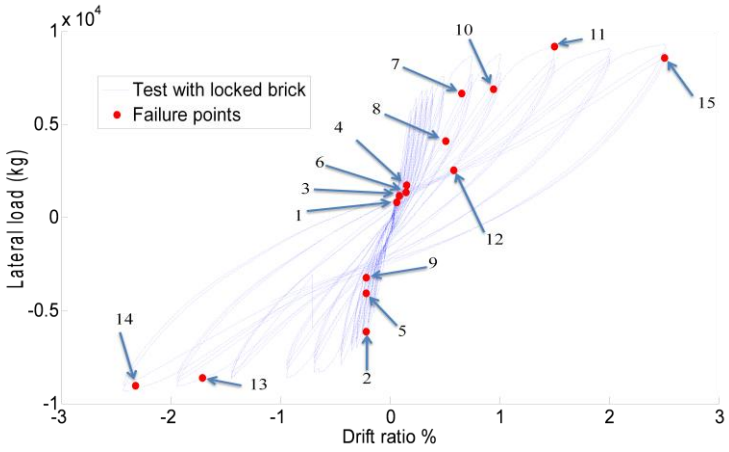

Figure 3.16 Drift ratio and lateral load values for each failure point in third test.

3.11 Discussion The Results

The main purpose from Implementation the bare RC frame is considering it as a control specimen with other tests which, infilled with different types of masonry clay bricks to understand the effect of the infill on the RC frame under earthquake. It should understand the effect of RC frame and sorthand it to understand the behavior of masonry infill wall by invesitigate the expermintal results of the bare frame and compering its results with standard brick infilled RC frame and locked brick infilled RC frame separately.

3.11.1 Comparing Bare Frame with Standard Brick Infilled RC Frame.

The profile and the parameters for the RC frame for each of bare RC frame and standard brick infilled RC frame is exactly the same with same protocol load and test setup just the difference between them is the second is infilled with standard clay brick. By studying the hysteretic curves for both of them together it should noticed that initial stiffness for infilled RC frame is become much bigger than the first test bare frame. Not just the initial stiffness, overall the lateral stiffness of RC frame is improved and it is need to apply more lateral load to get the aim displacement that because the strength of the frame structure is increased as shown in Figure 3.17. The comparison between the bare frame hysteretic response and standard brick infilled RC frame

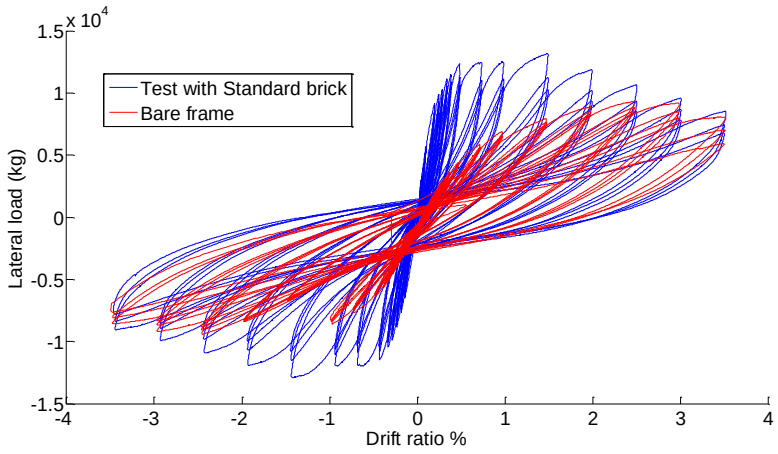

Figure 3.17 Comparison the hysteretic response between the bare frame and standard bricks infilled frame.

Investigating the Table 3.3 and Table 3.4 to know the difference between the failure types that occurred in each of them. the same failure types occurred in both of them but in different cycles, the failure's displacement value will be considered at the maximum cyclic value because the actual value that recorded in failure table represent the value of the researcher prediction in that time. So we cant consider it as a exactly value for the failure. Column bottom flexure failure is recorded for both specimens, in bare frame occurred in cyclic 63rd with cyclic maximum displacement value 4.41 mm and in the specimen with standard brick infill panel give the same failure in cyclic 89th with displacement cyclic maximum displacement value 10.13 mm. noticing that the same failure but with a big different values of displacements that the bare RC frame start much earlier from the infilled one. It should be mentioned that bar failed happened in bare frame test with displacement 48.88 mm considering it as the last failure occurred in bare frame test in the other hand this type of failure didn't noticed in standard infilled RC frame test.

3.11.2 Comparing Bare Frame with Locked Brick Infilled RC Frame.

The RC frames for both of bare frame and locked brick infilled RC frame (third test) have the same parameters with same load protocol and same test setup. But the result that got from the third test shows the different behavior especially at initial stiffness and load capacity. It is understood from the difference that got from the results that the infill is playing role by giving the the whole specimen improving at initial behavior. It can be understand the effect the behavior of the infill by studying the hysteretic response for both specimens together in Figure 3.18.

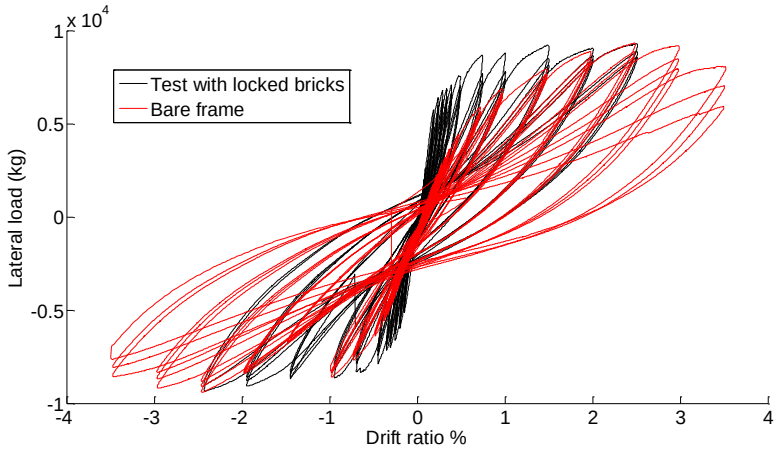

Figure 3.18 Comparison the hysteretic response between the bare frame and locked bricks infilled frame.

from the Figure 3.18 it is so clear that we lost the effect of the infill wall compeletly when the spicemen reached to cyclic number 108 in this cyclic the infill wall had the last failure compression crushing at the corner of the infill wall C3 after that the hysterestic response of the infilled frame behavior matched the hysteretic response for bare frame from this point on.

investigating the Table 3.3 and Table 3.5 to know the difference between the failure types that occurred in each of them. the same failure type occurred in both of them but in different Cyclic number. Column bottom flexure failure is recorded for both specimens but in bare frame occurred in cycle 63’rd with cyclic maximum displacement value 4.41 mm, and the specimen with standard brick infill panel gives the same failure in cycle 71’th with cyclic maximum displacement value 5.357 mm. From comparing the first failure displacement value for both of them it is clear that

the infill is improving the structure slightly. Bar failed is noticed in bare RC frame test and it was not recorded in locked brick infilled RC frame. The bar failed in bare frame is giving the proof that RC frame get tired much earlier than the infilled RC frame because of that it could not be noticed the bar failure in infilled specimens.

3.11.3 The Comparing Between RC Frame Infill with Standard Bricks and RC Frame Infill with Locked Brick.

In this section the effect of different types of brick infill on seismic load will be discussed. It was noticed that the behavior of the specimen with standard bricks was better than the specimen with locked as a lateral stiffness and load capacity. The standard brick shows bigger value with initial stiffness. The Figure 3.19 showing the hysteretic response for each of standard and locked infilled RC frames.

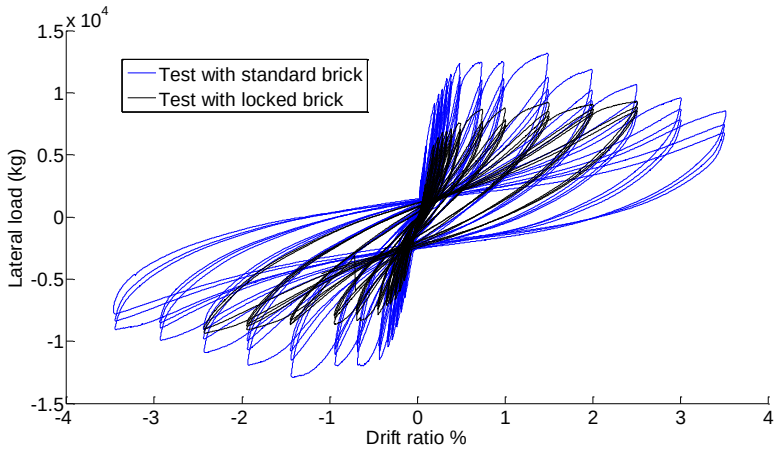

Figure 3.19 Comparison the hysteretic response between the standard and locked bricks infilled frames.

By studying the failure types and their displacement positions and lateral load values, it will be more clear to understand the behavior and the difference between their effect. The separation between the infill and the surrounding frame noticed to be the first failure type for both of them, following that cracking in the infill panel plaster. It can also possible to watch some levels of the test for each of specimens through Figure 3.20.

Standard bricks infilled RC Frame

Locked bricks infilled RC Frame

a) Drift ratio 0.3 %

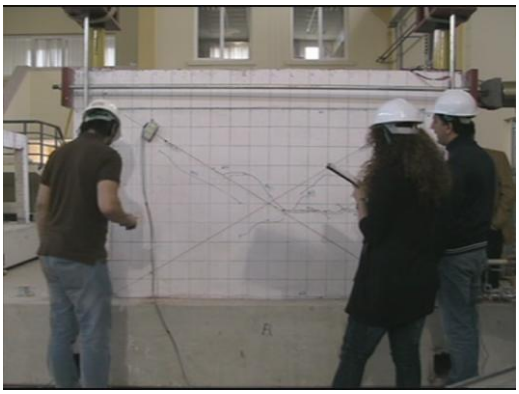

b) Drift ratio 0.5 %

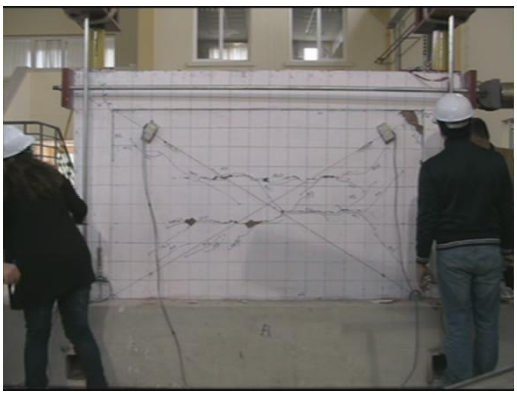

c) Drift ratio 0.75 %

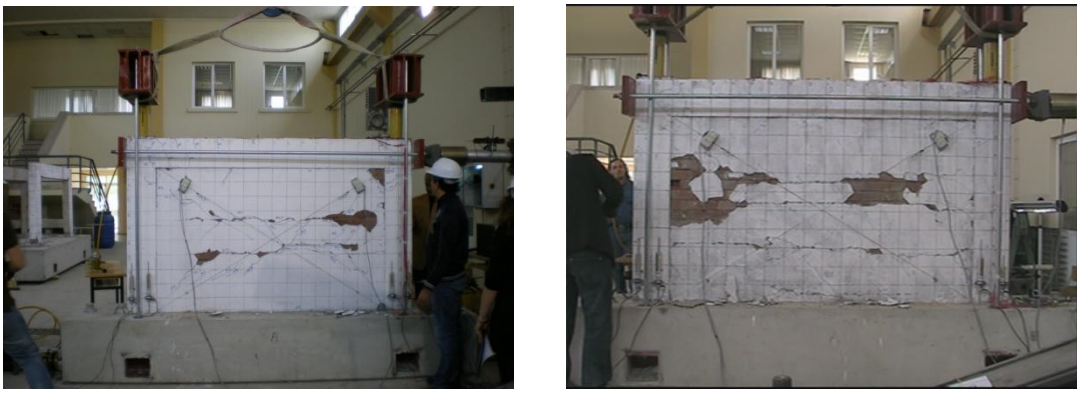

d) Drift ratio 1.0 %

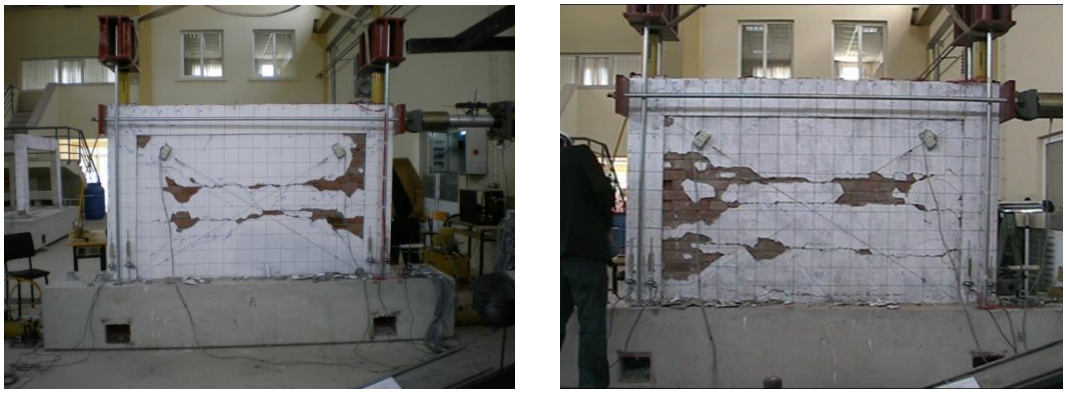

e) Drift ratio 1.5 %

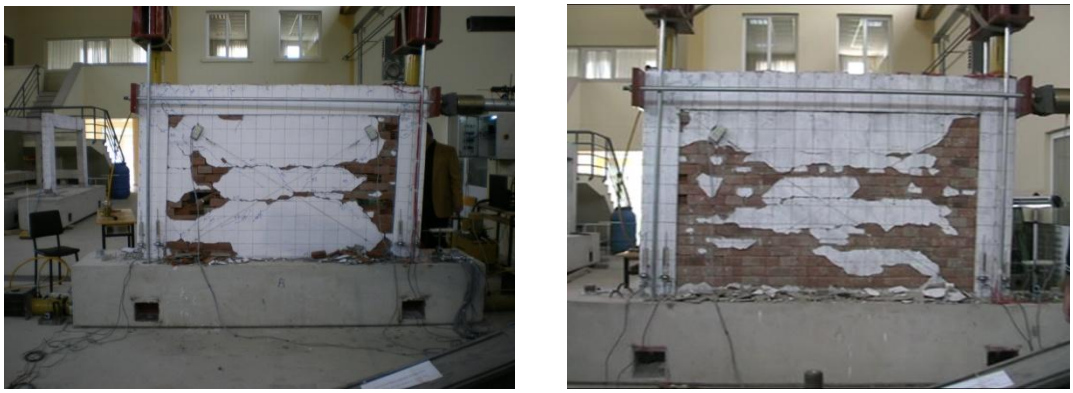

f) Drift ratio 2.5 %

g) Drift ratio 3.5 %

h) Test End

Figure 3.20 Exprimental work's levels showing different drift ratios % and the occurred failures in both standard and locked tests.

From Figure 3.20 it can be noticed the failure that happened at each test separately and study the failure that happening at the infill wall easily. The Figure 3.20a shows that the frame with locked brick gave the start failure with small cracks at infill plaster with drift ratio 0.3%. Figure 3.20b drift ratio 0.5% is showing that both of them have crack lines at the center of the infill. The spread of the cracks was more obvious with standard brick infill than the cracks at the locked brick by noticing the spreading of the line separating towards the corners at the standard bricks infill and all of that was recorded at drift ratio 0.75% in Figure 3.20c. Falling of plaster was recorded at Figure 3.20d with drift ratio 1.0% at each specimen but the fall that happened at locked infill was much more than falling in standard one and it is easier to be noticed at drift ratio 1.5% in Figure 3.20e. after cracks and falling of plaster at infill brick falling happened in wall with standard bricks but it didn't record any brick falling at wall with locked brick at drift ratio 2.5% showed in Figure 3.20f. falling lasted in standard bricks and exactly at the location that near to the columns with recording crushed corner but the situation was quite different at the wall with locked brick, it didn't suffered from any serious brick falling to the end of test Figure 3.20h.

By recording both of hysteretic response and the pictures for test levels for both of them, it can be noticed hystrertic response for standard, the wall was giving noticed resistance against the lateral load until drift ratio 2.5% and by compare it with captured picture with drift ratio 2.5% in Figure 3.20f. we understand that corner

crushing and bricks fall was the end of infill wall effect. By studying the hysteretic response for locked brick infilled RC frame, it so clear that the resistance of the infill wall was vanished after drift ratio 1.5% but from the figure 3.20 there were not any brick failure recorded the main reason was the special geometry that locked brick has see Figure 3.1a, it is understood form the name of locked brick that when the wall built the bricks are preventing each other from transverse movement because of the interaction between them.

As we discussed before that some displacement sensor are placed and also strain gauges. The strain value for each test that have recorded by strain gauges is close to each other Table 3.6 is showing the yield strain recorded at strain gauge no.14 at figure 3.3 column bottom with its drift ratio that occurred at.

Table 3.6 Strain and drift ratio

	Bare frame		**Standard infilled frame**		**Locked infilled frame**	
Drift ratio	0.9743	-0.9659	0.9392	-0.9805	0.7023	-0.7469
Strain	-0.002013	0.001925	-0.002519	0.002372	-0.002764	0.001387

The minus and the plus value of the strain in Table 3.6 represent the yield strain which the drift ratio and strain values behavior approximately linearly until this value after that the behavior is leaving the linearity see Figure 3.21

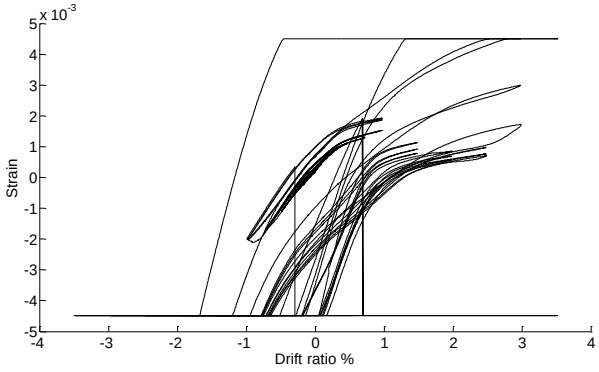

Figure 3.21 Drift ratio and strain.

CHAPTER FOUR

ANALYTICAL MODELING

4.1 Introduction

This chapter investigates techniques to analytically model composite RC frames. First, the modeling issues at the material and element level are addressed, using calibration studies on component tests that have been done in Dokuz Eylul University, Civil engineering department, structure mechanics laboratory, including reinforced concrete frame and masonry infill by using equivalent diagonal struts. While the focus of this chapter is on masonry infill by using equivalent diagonal struts, the results and guidelines can be applied to any systems that utilize these structural members (e.g. conventional all-RC frames with and without panels) and like investigating the effect of the soft storey in multi-storey building. Emphasis is placed on specific type of element model; a displacement derived beam-column element that is able to capture distributed plasticity by employing a fiber cross-section at integration points along the member. This model is used to analyze the single bay single storey test frame, and its response against the measured cyclic loading test data.

4.2 OpenSees Component Models

Open System for Earthquake Engineering Simulation (OpenSees) is a software framework for simulating the seismic response of structural and geotechnical systems (McKenna et al., 1999). OpenSees is an open source program that is continually evolving as researchers improve existing models and add new models and features. This section will specifically discuss the uniaxial materials and elements in OpenSees that can be used to represent the behavior of RC frame with and without infill panel under seismic load.

4.2.1 Material Models

The uniaxial material models are the most basic components in OpenSees to model a variety of force versus displacement (or stress versus strain) hysteretic responses. Material models can be used to make up the fiber cross-sections within beam-column elements (as described in Section 4.2.2). There are a number of material models provided in OpenSees. Three models are used in this study, the steel bar and types of concrete for the RC frame and masonry infill represented by struts.

Steel bar simulation is based on the Chang and Mander(1994) uniaxial steel model. The simulation has incorporated additional reversal memory locations to better control stress overshooting.

The backbone curve shown in Figure 4.1 is used as a bounding surface for the reinforcing bar simulation. This backbone curve is shifted as described by Chang and Mander (1994) to account for Isotropic hardening. This backbone can be obtained by utilizing simple tension test data. Within the material class, the backbone curve is transformed from engineering stress space to natural stress space (accounting for change in area as the bar is stressed.) This allows the single backbone to represent both tensile and compressive stress-strain relations. The tension and compression backbone curves are not the same in engineering stress space for this model. This transformation assumes small strain relations described by Dodd and Restrepo-Posada (1995).

The softening region (strain greater than eult), shown in Figure 4.1, is a localization effect due to necking and is a function of the gage length used during measurement. This geometric effect is ignored in this simulation. In this simulation, it is assumed that there is no softening in natural stress space. Because the simulation always converts back to engineering stress space, you will observe some softening in the tension response due to the reduction in area, however this will be much smaller than that shown in the original backbone curve proposed by Chang and Mander.

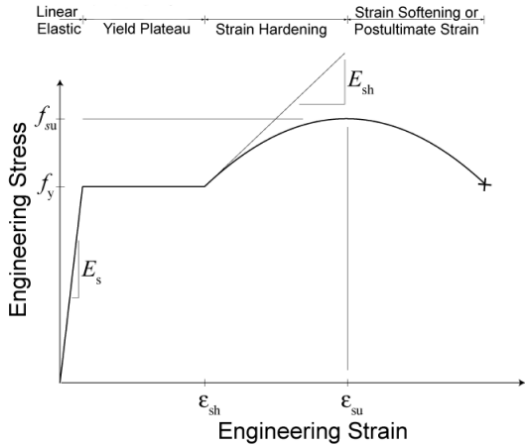

Figure 4.1 The backbone curve (Chang and Mander, 1994).

Cyclic degradation in this material is defined by three parameters first α is best obtained from calibration of test results. α is used to relate damage from one strain range to an equivalent damage at another strain range. This is usually constant for a material type. C_f is the ductility constant used to adjust the number of cycles to failure. A higher value for C_f the result will be in a lower damage for each cycle. A higher value C_f translates to a larger number of cycles to failure. C_d is the strength reduction constant. A larger value for C_d the result will be in a lower reduction of strength for each cycle. The four charts shown in Figure 4.2 demonstrate the effect that some of the variables have on the cyclic response. This material is referred to as ReinforcingSteel in OpenSees

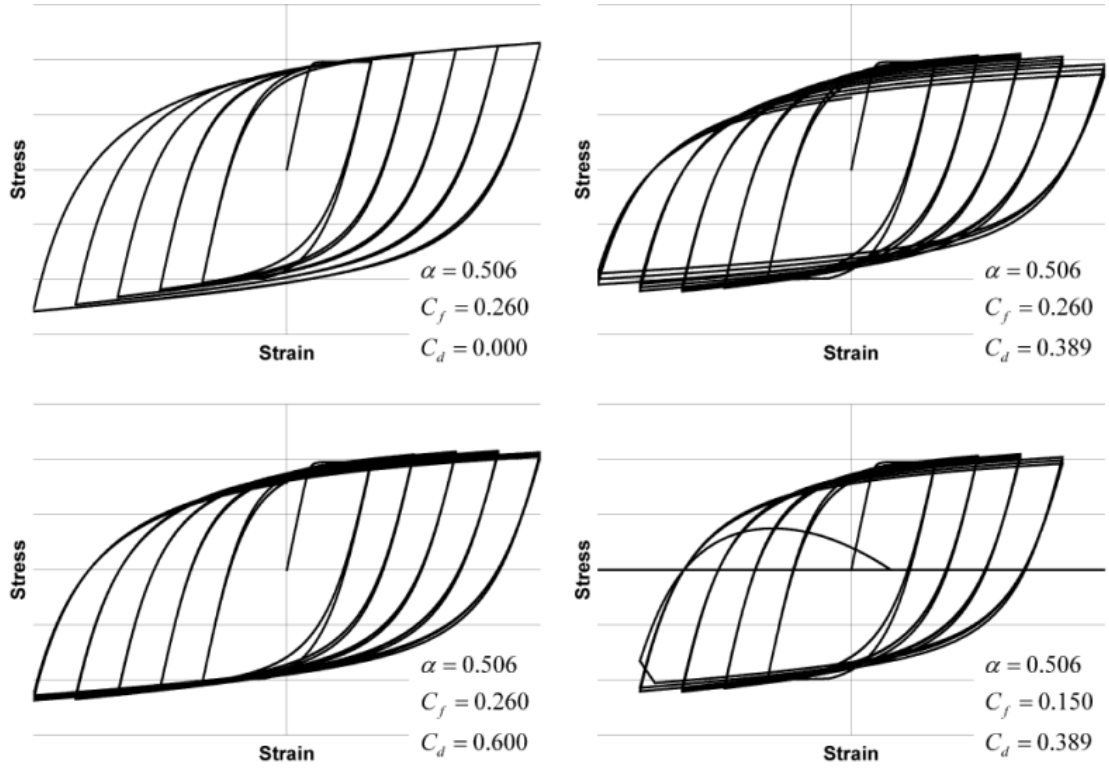

Figure 4.2 Fatigue and Degradation Parameter Examples.

The first type of concrete material model, which is used to represent the RC frames, is defined by the modified Kent and Park model (Scott et. al. 1982) and represents typical concrete crushing and residual strength behavior. It also allows for tensile strength with linear softening that helps to represent the interaction of the concrete and the reinforcement bars in tension Figure 4.3 the compression backbone of this model is defined by the points at which the material reaches the maximum crushing strength (f_{cc}', ε_{cc}) and the point when the residual strength attained (f_{c2}', ε_{c2}).

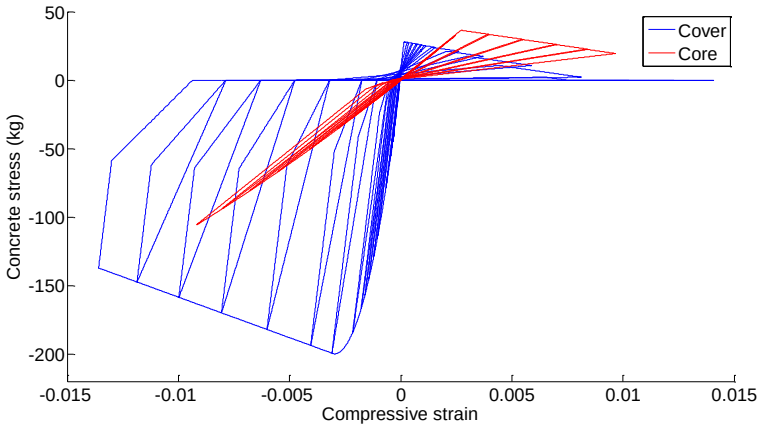

Figure 4.3 Hysteretic response for the OpenSees Concrete02 material model.

The tensile segment of the backbone is defined by the ultimate tensile strength (f_t) and the tensile softening slope is defined by (E_{ts}). This material model is referred to as Concrete02 in OpenSees.

The second type of concrete material model, which is used to represent the equivalent diagonal struts, defined by the modified Kent and Park model (Scott et. al. 1982) and represents typical concrete crushing and residual strength behavior but there is no tensile strength taken in consideration representing the real behavior of the infill panel. This material model is referred to as Concrete01 in OpenSees.

4.2.2 Displacement-Based Fiber Beam-Column Elements

There are several options in OpenSees to represent the nonlinear behavior of beam- column elements, one of which is the displacement-based element that can capture distributed plasticity with fiber cross-sections at a number of integration points along the element. The displacement-based formulation is based on linear displacement interpolation functions that accurately estimate the displacement distribution in members. This flexibility-based element is referred to as the DispBeamColumn in OpenSees. The fiber sections at each integration point represent the cross-section of the component being modeled i.e. reinforced concrete column and are composed of a mesh of fibers, each of which is assigned a uniaxial material hysteretic property (i.e. steel, concrete, etc.). In RC frames, these fiber sections are concrete models to represent material in the reinforced concrete beam and column.

4.2.2.1 Reinforced Concrete Frame

The reinforced concrete column fiber section is comprised of confined and unconfined concrete and steel reinforcement bars. The cover concrete, located outside of the transverse reinforcement, is considered as unconfined and will quickly begin to spall after reaching its crushing strength especially at columns bottom as have been recorded in chapter 3 in test works. The core concrete is confined on all sides by the longitudinal and transverse reinforcement and will behave in a more

ductile manner. Confined and unconfined regions are both modeled with the Concrete02 material in OpenSees (see Figure 4.3).

The compression backbone of the Concrete02 model can be defined according to the modified Kent and Park model (Scott et al. 1982), which adjusts the backbone parameters (f_{cc}', ε_{cc}, fc_2', ε_{c2}). This unaxial material is used to simulate the concrete in frame. The bare frame was used as a control specimen to understand the effect of the infill panel well from the other test so the parameters that have been used to represented and simulate the concrete in the bare RC frame it is the same in other tests. The characteristics that have been used in the Concrete02 cover and core concrete such as E_c (285000) and the rest as in Table4.1.

Table 4.1 Concrete01 parameters.

Variable Name	**Cover concrete**	**Core concrete**
$f_{cc'}$ (kg/ cm2)	200	260
ε_{cc}	0.003	$2x(f_{cc'}/E_c)$
$f_{c2'}$ (kg/ cm2)	$0.2x\ f_{cc}'$	$0.2x\ f_{cc}'$
ε_{c2}	0.01	0.02

The tensile cracking strength, f_t, of the core concrete is defined according to the following equation:

$$f_t = -0.14 \text{ x } f_{c'} \ (kg/cm^2) \qquad (4.1)$$

Where f_t and f_c' carry the unites shown. The tension stiffening effect is an important phenomenon that accounts for the interaction between the reinforcement bar and the surrounding concrete when subjected to tension. This effect provides a smooth transition in the moment curvature response by allowing the concrete to reach its maximum tensile stress and then slowly shedding the load until it reaches zero tensile strength. This effect has been modeled by Stevens et al. (1991) and can be represented linearly between zero and maximum tensile stress, beyond this point the stress decays as a function of the bar diameter and the ratio of total steel in the cross-section. Figure 4.4 depicts the typical tensile response of concrete accounting for this tensile stiffening effect. The concrete model in OpenSees allows one to model the tension strength decay using either an exponential decay, as suggested by Stevens (et al., 1991), or a linear decay.

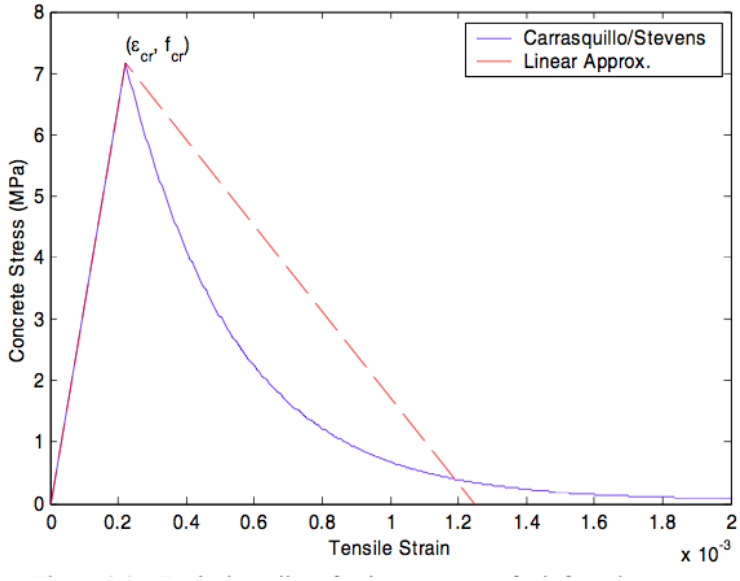

Figure 4.4 Typical tensile softening response of reinforced concrete, Cordova (2005).

The frame reinforcement steel can be modeled in OpenSees using the ReinforcingSteel material model, as described in section 4.2.1. The yield strength of the steel should either be taken from the measured value or as the expected yield strength, assumed equal to f_y. The initial stiffness of the steel is assumed E_s=2,100,000 kg/cm^2 and E_{sh}=0.0025xE_s. The yield strength is equal f_y=3400 kg/cm^2 and Ultimate stress in tension is f_u=6000 kg/cm^2. According to strains value, Strain corresponding to initial strain hardening is equal e_{sh}=0.004 and the Strain at peak stress e_{ult} =*0.019*. In this modeling Coffin-Manson Fatigue and Strength Reduction α, C_f and C_d are with values respectively 0.502, 0.260 and 0.389 is the only one which, taken in consideration besides ignoring the other optional parameters.

4.2.2.2 Infill Strut

Infill walls in the tests that have been done in Dokuz Eylul University, Civil engineering department, structure mechanics laboratory can be generally categorized into 2 types first standard brick the second locked brick and both of them are considered as hollow clay bricks. The compression strength of the masonry prism, f_p, is determined from an equation recommended by Paulay and Priestly (1992) as:

$$f_p^{'} = \frac{f_{cb}^{'}(f_{tb}^{'} + \alpha f_j^{'})}{U_u(f_{tb}^{'} + \alpha f_{cb}^{'})}, \quad \text{where} \quad \alpha = \frac{j}{4.1 h_b}, \quad \text{and} \quad U_u = 1.5 \qquad (4.2)$$

A masonry infill panel can be modeled by replacing the panel with a system of, diagonal masonry compression struts. By ignoring the tensile strength of the infill masonry, the combination of both compression components provides a lateral load resisting mechanism for the opposite lateral directions of loading. Compression failure of infill walls occurred due to the compression failure of the equivalent diagonal strut. The equivalent strut width Z, in Figure 4.5, is computed using a modification recommended by FEMA 306 (1998).

$$V_c = ztf_m^{'} cos\theta \qquad (4.3)$$

and Z equivalent strut width obtained by the following equation FEMA 306 (1998):

$$Z = 0.175(\lambda h)^{-0.4} d_m \qquad (4.4)$$

where

$$\lambda = \left[\frac{E_m t sin 2\theta}{4E_c I_g h_m}\right]^{\frac{1}{4}} \qquad (4.5)$$

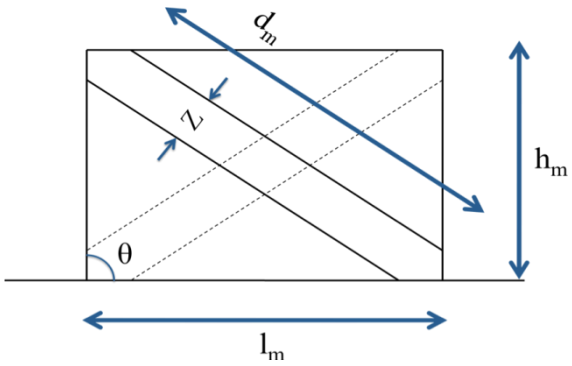

Figure 4.5 the equivalent diagonal compression action parameters.

h column height between centerlines of beams, h_m height of infill panel, E_c expected modulus of elasticity of frame material, =285000 kg/ cm^2, E_m expected modulus of elasticity of infill material equal to $750f_m$, Paulay, and Priestley, (1992). I_g moment of inertial of column, d_m diagonal length of infill panel, t thickness of infill panel and

equivalent strut (all the units in kg and cm), θ angle whose tangent is the infill height to-length aspect ratio, as :

$$\theta = tan^{-1}\left(\frac{h_m}{l_m}\right) \qquad (4.6)$$

where l_m length of the infill panel

The compression backbone of the Concrete01 model can be defined according to the modified Kent and Park model (Scott et al. 1982), represents typical equivalent diagonal strut crushing and residual strength behavior but there is no tensile strength is considered which adjusts the backbone parameters (f_{cc}', ε_{cc}, f_{c2}', ε_{c2}). This unaxial material is used to simulate the concrete in the infill strut.

4.3 Comparison The Analytical Results to Experimental Response

Over twenty five data channels were recorded during the test for the bare frame and more for the tests with infill panel, with a large majority of these dedicated to tracking the response of the infill panel, joints, columns and foundation movement. This section will extract a couple of the hysteretic response of the bare and infilled RC frame plots for the tests under cyclic load event and compare them to the analytical results predicted by OpenSees. The first test bare was considered as the control test to understand the behavior of the RC frame under cyclic load.

4.3.1 Modeling of Bare Frame

The reinforced concrete bare frame are modeled using the displacement-based fiber elements described in Section 4.2.2. The RC fiber section can be defined using three different materials to represent the core and cover concrete and the reinforcement steel. The Concrete02 material model is used to represent both the core and cover concrete. Based on the calibration study presented in Section 4.2.2.1, it is recommended to specify the nominal compressive strength in the modified Kent and Park model as 1.3 *fc* and it is the ratio of confined to unconfined concrete strength, since the full *fc* was found to provide a better estimate of the strength for

cover concrete of the tests considered in the calibration study. The backbone of the cover concrete is defined according to the following backbone parameters: *fcc*'=200 kg/cm^2 ε_{cc} =-0.003, f_{c2}'= 0.2 f_{cc}', and ε_{c2}= -0.010.

It is recommended that the longitudinal reinforcement steel be modeled using the ReinforcingSteel material model in OpenSees. All the values of this material discussed in the section 4.2.2.1 used to model the bar steels in the bare RC frame and it summarized in Table 4.2 for all the tests.

Table 4.2 Summary of OpenSees input parameters for definitions of ReinforcingStee material.

Variable Name	bare frame	S. B. infilled RC frame	L.B. Infilled RC frame
E_s	2100000	2100000	2100000
E_{sh}	0.0025 E_s	0.0025 E_s	0.0025 E_s
F_y	4200	4200	4200
F_u	6000	6000	6000
e_{sh}	0.004	0.004	0.004
e_{ult}	0.019	0.019	0.019
α	0.502	0.502	0.502
C_f	0.26	0.26	0.26
C_d	0.389	0.389	0.389

The hysteretic response comparing between test and the OpenSees results shown in Figure 4.6. The OpenSees response is represented as a dashed red line while the measured test response is shown as a solid blue line.

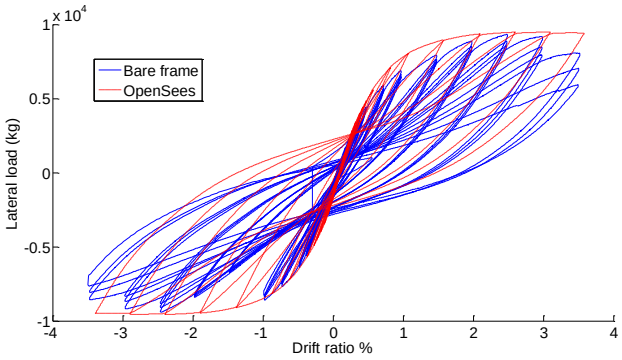

Figure 4.6 Calibration the hysteretic response for the RC bare frame by OpenSees.

4.3.2 Modeling of Frame Infilled with Standard Brick

The same parameters that have been taken in the first test for the bare RC frame are considered the same for second test, RC frame with standard brick infill. The infill panel in the second test is represented by two equivalent diagonal struts. The characteristics of the diagonal struts take the same characteristics of the masonry prism by ignoring the occurring friction between the infill wall and the surrounding frame. The compression strength of the masonry prism, f_p, is determined from an equation 4.2.

The elasticity modulus of infill panel can be calculated as 750 f_p =16410 kg/cm^2 Paulay, and Priestley, (1992). Compression failure of infill walls occurred due to the compression failure of the equivalent diagonal strut. The equivalent strut width Z, in Figure 4.5, is computed using equation 4.4.

The compression backbone of the Concrete01 model is used to simulate the equivalent diagonal strut and ignore the tensile strength of the infill masonry and represent the crushing and residual strength behavior. the parameters in the backbone parameters (f_{cc}', ε_{cc}, f_{c2}', ε_{c2}) is summarized in Table 4.3.

Table 4.3 Summary of OpenSees input parameters for definitions of the equivalent diagonal strut represented by Concrete01 in the second test, standard brick infilled RC frame.

Variables Name	**Standard brick infill**
E_m	16500 kg/cm2
f_p	22 kg /cm2
f_{pu}	0.02 f_p
e_p	0.002
e_{pu}	0.013
Z	25 cm

The hysteretic response comparing between the second test and the OpenSees results shown in Figure 4.7. The OpenSees response is represented as a dashed red line while the measured test response is shown as a solid blue line.

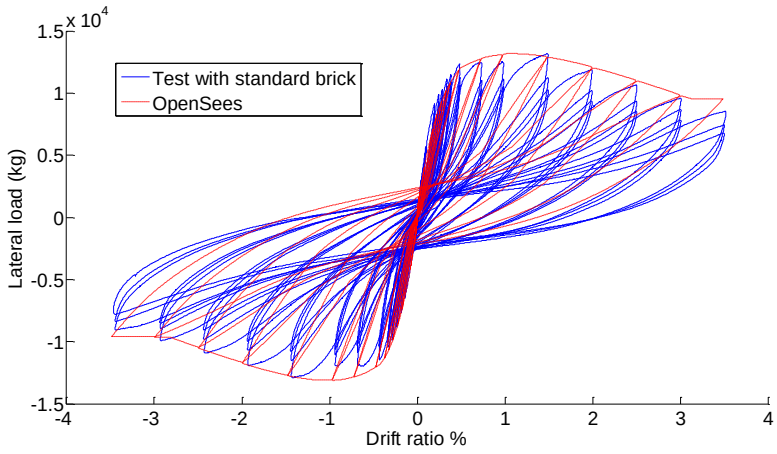

Figure 4.7 Calibration the hysteretic response for the RC frame with standard brick infill by OpenSees.

4.3.3 Modeling of Frame Infilled with Locked Brick

The same parameters that have been taken in the first and the second test for the RC frame are considered the same for third test, RC frame with locked brick infill. Two equivalent diagonal struts represent the infill panel in the third test. The characteristics of the diagonal struts take the same characteristics of the masonry prism by ignoring the occurring friction between the infill wall and the surrounding frame. The compression strength of the masonry prism, f_p, is determined from an equation 4.2.

The elasticity modulus of infill panel can be calculated as 750 f_p =7524 kg/cm^2 Paulay, and Priestley, (1992). Compression failure of infill walls occurred due to the compression failure of the equivalent diagonal strut. The equivalent strut width Z, in Figure 4.5, is computed using equation 4.4.

The compression backbone of the Concrete01 model is used to simulate the equivalent diagonal strut and ignore the tensile strength of the infill masonry and represent the crushing and residual strength behavior. The parameters in the backbone parameters is (f_{cc}', ε_{cc}, f_{c2}', ε_{c2}) summarized in Table 4.4.

Table 4.4 Summary of OpenSees input parameters for definitions of the equivalent diagonal strut represented by Concrete01 in the third test, locked brick infilled RC frame.

Variables Name	**Locked brick infill**
E_m	7500 kg/cm2
f_p	10 kg /cm2
f_{pu}	0.02 f_p
e_p	0.0015
e_{pu}	0.006
Z	25 cm

The hysteretic response comparing between the second test and the OpenSees results shown in Figure 4.8. The OpenSees response is represented as a dashed red line while the measured test response is shown as a solid blue line.

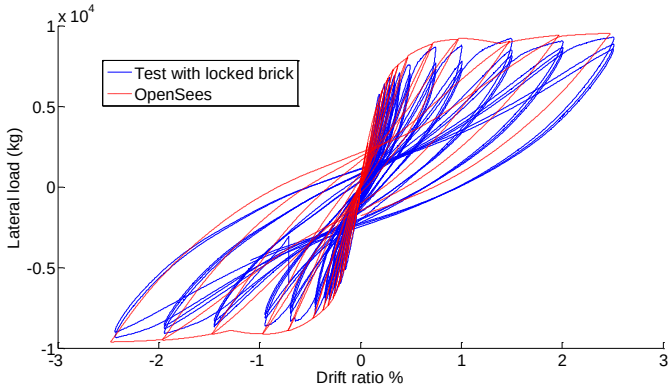

Figure 4.8 Calibration the hysteretic response for the RC frame with locked brick infill by OpenSees.

4.4 The Effects of Number of Bays and Infills Materials on Structure Lateral Behavior

In the Figure 4.9 the hysteretic envelope obtained from single bay in the blue line and the dashed red one for the two bays and both of them bare RC frame. In Figure 4.10 the hysteretic response obtained from single bay in blue line and the dashed red one for the two bays and both of them RC frame infilled with standard brick. The Figure 4.11 is showing the hysteretic response for single and two bays for locked brick infilled RC frames.

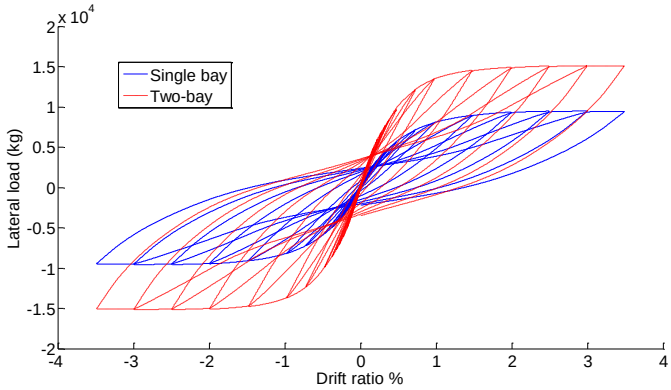

Figure 4.9 Bare RC frame single and two bays hysteretic response comparison.

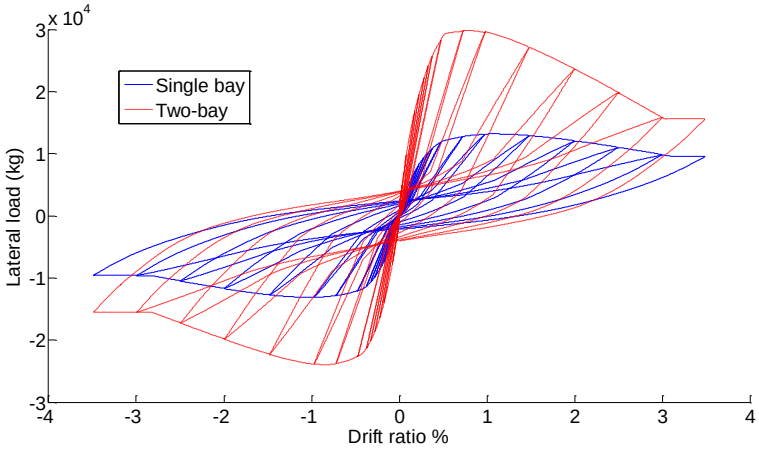

Figure 4.10 Standard brick infilled RC frame single and two bays hysteretic response comparison.

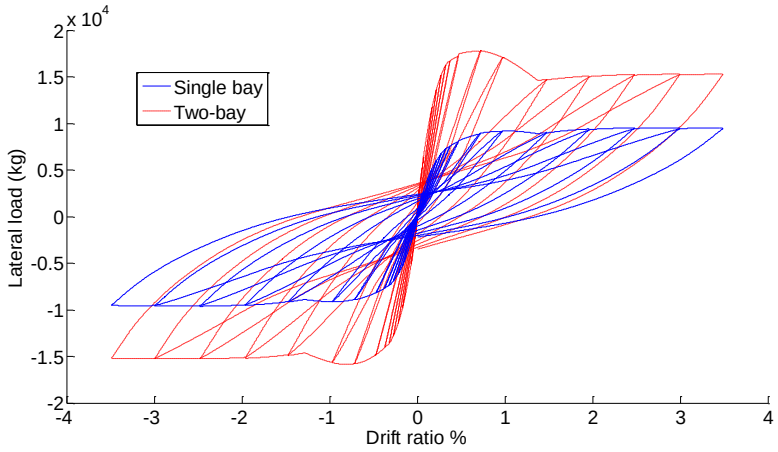

Figure 4.11 Locked brick infilled RC frame single and two bays hysteretic response comparison.

From Figures 4.9, 4.10 and 4.11 we understand that the increasing in number of bay has significant effect in lateral stiffness and the capacity (ultimate load) for the two-bay increased about 50% more than the capacity that obtained from the single-bay.

To understand the role of infill panel for each of standard and locked infill Figure 4.12 and 4.13 demonstrated the effect of the infill, standard and locked respectively through two-bays by comparing bare and the infilled frame together.

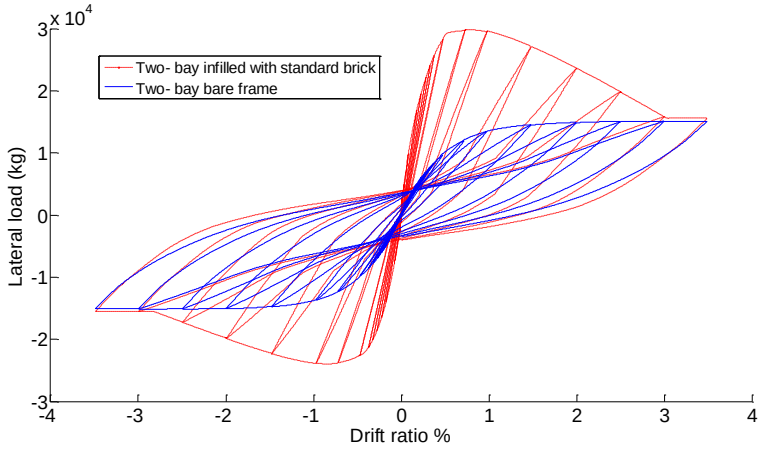

Figure 4.12 Behavior of the standard brick infill panel inside two-bay RC frame.

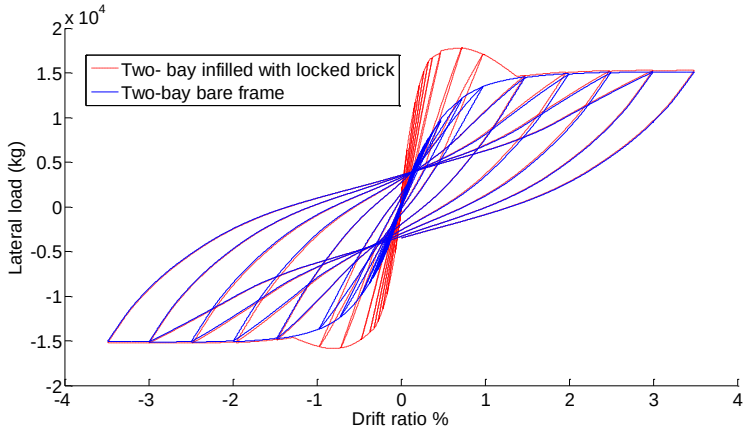

Figure 4.13 Behavior of the locked brick infill panel inside two-bay RC frame.

From Figures 4.12 and 4.13 noticing that the effect at initial stiffness is significant at both of them but the increasing that obtained from standard infilled specimen much more than the increasing that obtained from the specimen infill with locked brick. The ultimate capacity for the standard brick infilled RC frame reaches 25 ton.

4.5 The Effect of The Soft Storey

Has been noticed that most of the multi-stories building exhibit soft-storey (see Figure 4.14). Soft storey is one of the most common causes of failure in earthquake because the first stories have feature relatively large window and door openings and fewer partitions (less bracing) than the other stories where the bedrooms and bathrooms are located. In pervious sections from this chapter calibrating has been done form experimental results and modeled by OpenSees. From the modeling and analytical study for single bay single storey we will try to understand the effect of the soft first-storey behavior.

Figure 4.14 Typical building with a soft ground storey in India (EERI 2001).

At simulate a multi-storey building the procedure of applying cyclic is different from applying cyclic at single-storey. As we discussed that before that the applied cyclic load at single bay was at the side of top node of frame but the situation is different at multi-storey the applied cyclic load is represented as triangle by the ratio of weight each floor (see Figure 4.15c).

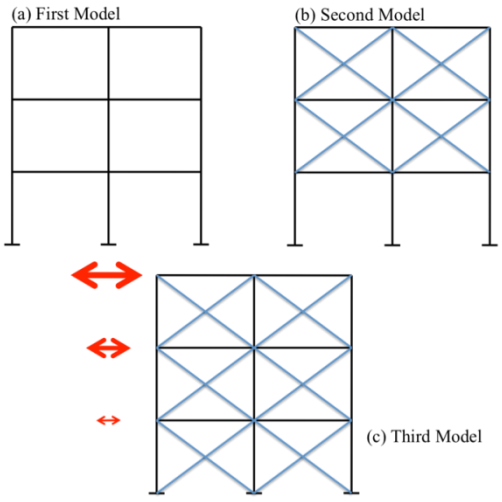

Figure 4.15 Structure Models.

Three different models are in the Figure 4.15 the first model a represent building without infill walls consist of three storey, the second model b represent building with bare ground storey and the third model c represent building with infill wall at three storey. To understand the effect of the bare storey and infill panels, hysteretic response of each model has been modeled by using the same parameters that we get

from calibrating the tests in OpenSees. In the Figure 4.16 and 4.17 second and third model are simulated the effect of the bare ground storey at the building infilled with standard brick and locked brick respectively. The blue line represents the building with bare storey the second model and the red dashed line represents third model.

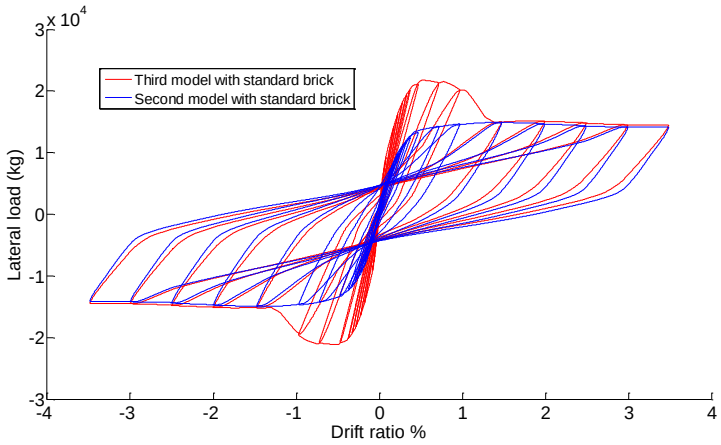

Figure 4.16 Hysteretic response for the second and the third model infilled with standard brick.

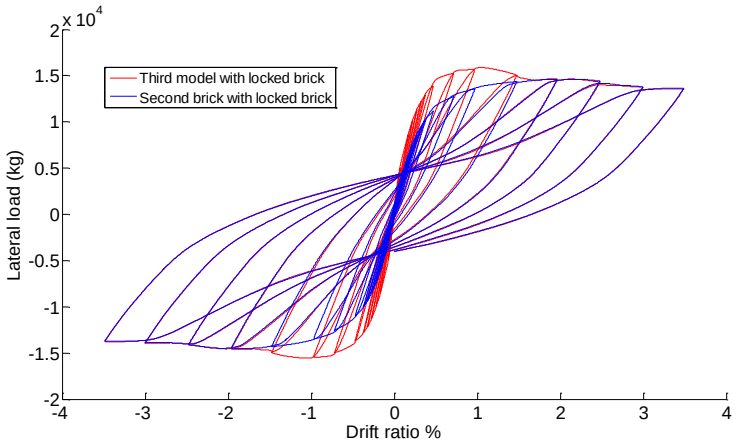

Figure 4.17 Hysteretic response for the second and the third model infilled with locked brick.

From the Figures 4.16 and 4.17 it is so clear to notice the effect of the bare storey at whole building behavior under seismic load. The big effect that bare storey has comes from the plastic hinge that occurring usually at the first floor according to geometry of the building. The infill panel at first floor gives the whole structure increasing at initial stiffness (see Figure 4.16 and 4.17).

By comparing the hysteretic response for the second and third model we notice the big different between them as we discussed this before. To understand if there is any effect comes from the infill panels that located at the upper stories like the second model the building with bare ground storey, Figure 4.18 and 4.19 inform the behavior of the infill panels at upper stories (with bare ground storey) and how much effect is generated under seismic load by comparing it with bare model (first model). The Figure 4.18 and 4.19 for the systems infilled with standard and locked brick respectively represented in red dashed line and the blue line for the first model (bare system).

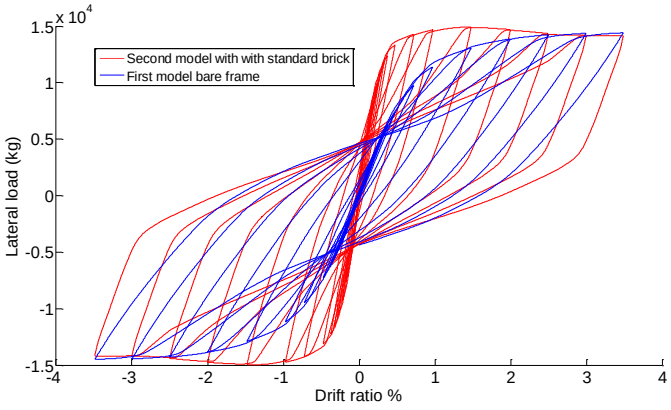

Figure 4.18 Hysteretic response for the first and the second model both of them infilled with standard brick.

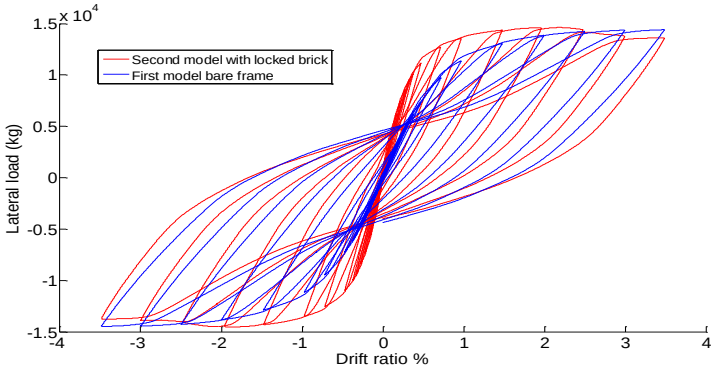

Figure 4.19 Hysteretic response for the first and the second model infilled with locked brick.

Although the effect of the infill decreased too much in building with bare storey, noticeable increasing recorded at the initial stiffness for each of the system that infilled with standard brick and the system with locked brick infill.

Form comparing between the three models, we noticed that the different between model with first bare storey and totally infilled with the standard infill is big, Figure 4.16. The case in second model is different which mean the more stiffness that the brick shown the more difference in lateral force that between the first bare storey and the upper storey is generating the more damage that the building will suffer from. The building will be more stabile if the behavior of hysteretic response for building with second model and bare building is close see Figure 4.18 and Figure 4.19. The behavior of the building with locked brick is better than the behavior of the building with standard brick. So the building with locked brick is safer under lateral load. So it should to whether there any risk form being the first storey is bare and consider it as a soft storey or not and that by applying Equivalent seismic load method

4.5.1 Equivalent Seismic Load Method

After investigating and study the first bare storey case for the three storey-two bay modeled by OpenSees under cyclic load, it was noticed that when the model with bare first floor gives different behavior so it should understand whether the model is considered with soft storey or not by using equivalent seismic load method.

Equivalent seismic load method is trying simulating earthquake load on the model by applying static load on each storey of the building. The first period that we need in equivalent seismic method to calculate T_1 is calculated by OpenSees. After that F_1, F_2, F_3 (see Figure 4.20) that representing the static load at each floor and from these static loads, displacements are taken to be substituted in Equation 4.7 later.

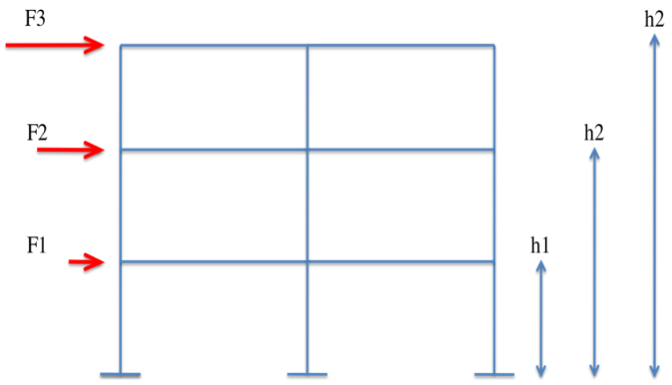

Figure 4.20 Applying the static load at each storey.

The case where in each of the two orthogonal earthquake directions, Stiffness Irregularity Factor η_{ki} , which is defined as the ratio of the average storey drift at any storey to the average storey drift at the storey immediately above and it is calculated by the Equation 4.7. Whether the results is greater than 2 than the building or the model is considered with soft storey.

$$\eta_{ki} = (\Delta_i / h_i) / (\Delta_{i+1} / h_{i+1}) > 2.0 \qquad (4.7)$$

After finding the values of the displacements at each storey after applying the static load by Equivalent seismic load method Table 4.5 showing the results and the value of the factor for 4 models.

Table 4.5 Stiffness irregularity factor.

Variable	**RC frame infilled with standard brick**	**RC frame infilled with locked brick**	**Soft storey case**	
			RC frame infilled with standard brick	**RC frame infilled with locked brick**
T	0.1164	0.26424	0.36636	0.37998
V_t	4036	3867	3867	3867
F_1	790	755	755	755
F_2	1580	1512	1512	1512
F_2	1580	1512	1512	1512
η_{ki}	0.838	0.917	1.456	1.242

The Stiffness Irregularity Factor η_{ki} for the both of models that infilled with locked and standard brick are not greater than 2, so both of them are not considered with soft storey but by comparing between the results in Table 4.5 for each of model with first bare storey, we notice that the model with locked brick gives better results in terms of soft storey criteria because it is smaller than 1.456 and farther from 2 by comparing it with model that infilled with standard brick.

CHAPTER FIVE

CONCLUSION AND RECOMMENDATIONS

This study assesses the seismic performance of masonry-infilled RC frames, including a set of three specimens single bay single storey with different infill configurations under experimental and analytical investigations. Infill panels are modeled by two nonlinear strut elements, which only have compressive strength. Nonlinear models of the frame-wall system are subjected to incremental dynamic analysis in order to assess seismic performance. Simulations were performed through a nonlinear finite element program, Opensees. With the application of the strut model it is possible to give good solution for infill frame evaluation. The experimental and simulation results both of them show that the presence of masonry infill walls can affect the seismic behavior of framed building to large extent. These effects are generally positive: masonry infill walls can increase global stiffness and strength of the structure. The energy dissipation capacity of the frames with infill walls is higher than that of the bare frame. The better collapse performance of fully-infilled frames is associated with the larger strength and energy dissipation of the system for instant the infill with standard brick whereas the infill with locked brick suffered less than standard brick.

5.1 Limitations and Errors

The more complex test you have done the more limitations and errors you got. In these test that have been done in Dokuz Eylul University, structural mechanics laboratory some limitations errors were recorded after investigating the results.

Displacement sensors and strain gauges were setup on specimens to measure each of displacement and reinforcement steel strain. The values that we obtained from displacement sensors were successfully recorded and accurate but the results that be

obtained from strain gauges had some limitations and this because lack informations in setup and calibrate the gain of the strain gauge by choosing the wrong range of gain values. Gain values that have been chosen was the maximum 885-889 to increase the accuracy and be able to read the initial values clearly, as a results the strain gauges could not able to recode the big values so the maximum strain values is not known see Figure 5.1 and Figure 5.2.

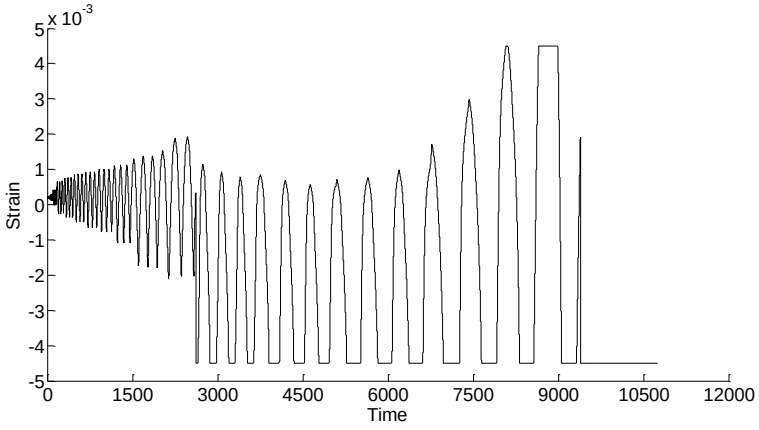

Figure 5.1 The time history of steel strain.

As is showen in Figure 5.1 the biggest value that the strain gauges could record was 0.005 and the bigger values were not recorded so it is not possible to read and understand the behavior of reinforcement steel at big values.

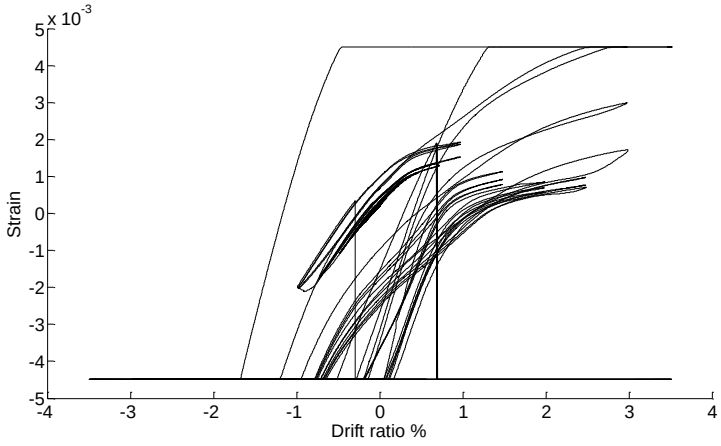

Figure 5.2 Drift ratio and strain relationship.

The initials values at Figure 5.2 shown that the behavior is approximately linear between Drift and steel strain and that was expected because the more drift is applied the more strain is being obtained but the values is limited by 0.005 so it is possible to read the bigger values.

Some limitation recorded from modeling the RC frame infilled with masonry infill by using OpenSees. The main limitation in OpenSees program that it can not represent the infill panel just as two equivalent diagonal struts, as results the friction that cause between the infill panel and the surrounding frame is being ignored by using struts and that decrease the realistic that we are looking for. The computer programs are not able to simulate the failure and showing damages maps specifically. Losing the ability to specify the failure and its time in computer programs made it impossible to compare the details for the behavior experimental tests so it is just possible to compare general information that obtained from the simulation.

5.2 Recommendations for Future work

Further studies will examine the effect of other types of masonry materials on seismic performance, and evaluate the behavior of frames with stronger like using reinforcement system walls and infill with openings for windows and doors. Avoid the limitation and errors that happened with measuring steel strain and that by decreasing the value of gain and use the value with middle range 492 to 498 to get better results and be able to read the maximum values of steel strain

REFERENCES

Ambrisi, A.D. & Filippou, F.C. (1999). Modeling of Cyclic Shear Behavior in RC Members. *Journal of Structural Engineering, Vol. 125, No.10.* 1143-1150.

Bell, D.K. & Davidson, B.J. (2001). *Evaluation of earthquake risk buildings with masonry infill panels*. Paper No.4.02.01. University of Auckland.

Calvi, G.M., Bolognini, D. & Penna, P. (2004). *Seismic performance of masonry - infilled RC frames*. University of Pavia. 254-275.

Cesar, M.T., Oliveira, D. & Barros, R.C. (2008). Comparison of cyclic response of reinforced concrete infilled frames with experimental results. *The 14'Th World Conference on Earthquake Engineering*, Beijing, China.

Chang, G. and Mander, J. (1994). "Seismic Energy Based Fatigue Damage Analysis of Bridge Columns: Part I – Evaluation of Seismic Capacity." NCEER Technical Report 94-0006.

Cordova P.P. & Deierlein G. G. (2005). Validation of The Seismic Performance of Composite RCS Frames. *Report No. 155, John A. Bulme Earthquake Engineering Center*, Department of Civil and Environmental Engineering, Stanford University. Stanford, CA.

EERI (2001). *Preliminary Observations on the Origin and Effects of the January 26, 2001 Bhuj (Gujarat, India) Earthquake*. EERI Newslettres, Vol. 35, N°. 4; Oakland

FEMA-306 (1999). Evaluation of Earthquake damaged concrete and masonry wall buildings – Basic Procedures manual. *Federal Emergency Management Agency*, Washington, D.C.

FEMA 356 (2000). Prestandart and Commentary for the Seismic Rehabilitation of Buildings. *Federal Emergency Management Agency*. Washington DC.

Karayannis, Ch. G., Kakaletsis, D. J. & Favvata, M.J. (2005). Behavior of bare and masonry infilled R/C frames under cyclic loading: Experiments and analysis. *WIT Transactions on The Built Environment, Vol 81. Democritus University of Thrace*, Greece. 429-438.

Kermani, A.M., Goldsworthy, H.M. & Gad, E.F. (2008). A review of the seismic behaviour of RC frames with masonry infill. *University of Melbourne*, Parkville, Australia.

Kermani, A.M., Goldsworthy, H.M. & Gad, E.F. (2008). The behaviour of RC frames with masonry infill in wenchuan earthquake. *University of Melbourne*, Australia.

Korkmaz, K.A., Demir, F. & Sivri, M. (2007). Earthquake assessment of RC with masonry infill walls. *International Journal of Science & Technology, Vol 2 No 2.* 155-164.

Marjani, F. & Ersoy, U. (2002). Behavior of brick infilled reinforced concrete frames under reversed cyclic loading. *ECAS2002 International Symposium on Structural and Earthquake Engineering*, METU, 142-150.

McKenna, F. and Fenves, G. L. (2001). "http://opensees.berkeley.edu. The OpenSees command language primer". Department of Civil and Environmental Engineering, University of California, Berkeley, CA.

Ministry of Public Works and Settlement. (2009). *Specification for Structures to be Built in Disaster Areas.* IMO/09/01. Turkey

Mosalam, K.M., White, R.N. & Gregely, P. (1997). Static response of infilled frames using quasi-static experimentation. *Journal of Structure Engineering, Vol. 123, No. 11.* 1462-1469.

Mostafaei, H. & Kabeyasawa, K. (2004). Effect of infill masonry walls on the seismic response of reinforced concrete buildings. *Tokyo University Earthquake Research Institute, Vol 79,* Tokyo, 133-156.

Pauley, T. & Priestly, M.J.N. (1992). Seismic design of reinforced concrete and masonry buildings. John Wiley & Sons, Inc.

Pujol, S., Climent, A.B., Rodriguez, M.E., & Pardo, J.P. (2008). Masonry infill walls: An effective alternative for seismic strengthening of low-rise reinforced concrete building structures. *The 14'Th World Conference on Earthquake Engineering,* Beijing, China.

Srinivas, B & Prasad, B.K. (2005). The influence of masonry infill in reinforced concrete multi-storey buildings to near-fault ground motions. *Indian Institute of Science,* India.

Taher, S.F. & Afefy, H.M. (2008). Roll of the masonry infill on seismic resistance of RC structure. *Arabian Journal for Science and Engineering, Vol 33 No 2B.* 261-306.

Tuladhar, P. & Kusunoki, K. (2006). Seismic design of the masonry infill RC frame buildings with first soft storey. *Dept. of Urban Development & Building Construction*, Nepal.

Vaseva, E. (2009). Seismic analysis of infilled RC frames with implementation of a masonry panel models. *11'Th National Congress on Theoretical and Applied Mechanics,* Vol 2 No 5. Bulgaria.

APPENDICES

NOTATION

C_f Coffin-Manson constant

C_d Cyclic strength reduction constant

d_m Diagonal length of infill panel

E_c Modulus of elasticity for concrete

E_{ts} Concrete tension softening stiffness

E_s Modulus of steel

E_{sh} Tangent at initial strain hardening

E_m Modulus of elasticity of infill material

e_{sh} Strain corresponding to initial strain hardening

e_{ult} Strain at peak stress

F_1 Design seismic load acting at 1.st storey in Equivalent Seismic Load Method

F_2 Design seismic load acting at 2.nd storey in Equivalent Seismic Load Method

F_3 Design seismic load acting at 3.rd storey in Equivalent Seismic Load Method

f_{cc}' Concrete compressive strength

f_{c2}' Ultimate compressive strength for concrete

f_t Concrete tensile strength

f_y Yield stress in tension for reinforcement steel

f_u Ultimate stress in tension

f_p Masonry prism compressive strength

f_{cb} Compressive strength of the brick

f_{tb} Tension strength of the brick

f_j Mortar compressive strength

f_m Masonry compression strength

h Column height between centerlines of beams

h_m Height of infill panel

I_g Moment of inertia for columns

j The mortar joint thickness

l_m Length of infill panel

T Building natural vibration period [s]

t Thickness of infill panel and equivalent strut

U_u The stress non-uniformity coefficient

V_c Shear force (Horizontal component of the diagonal strut capacity)

V_t In the Equivalent Seismic Load Method, total equivalent seismic load acting

Z Equivalent strut width

α Coffin-Manson constant

ε_{cc} Concrete strain at maximum compressive strength

ε_{c2} Concrete strain at ultimate compressive strength

θ Angle whose tangent is the infill height-to-length aspect ratio

η_{ki} Stiffness Irregularity Factor defined at i'th storey of building

Δ_i Storey drift of i'th storey of building

LIST OF FIGURES

LIST OF TABLES

OPENSESS SCRIPT

Reinforced Concrete Frame

```
default -Length cm -Force kgf -Time sec
source setUnits.tcl
source BuildRCrectSection.tcl;          # procedure for defininig RC fiber section
set dataDir databir1;                   # set up name of data directory
file mkdir $dataDir;                    # create data directory
# define GEOMETRY -------------------------------------------------------------
# nodal coordinates:
# Create Elastic material prototype - command: uniaxialMaterial Elastic matID E
# uniaxialMaterial Elastic 1 285000.
# For BeamColumn Members
    model basic -ndm 2 -ndf 3;      # 2 dimensions, 3 dof per node
    node 1 0 0;                 # node#, X Y
    node 2 200 0;
    node 3 0 137.5;
    node 4 200 137.5;
    set LCol 137.5;
# Define materials for frame elements
    set IDconcCore 2;           # material ID tag -- unconfined cover concrete
    set IDconcCover 3;          # material ID tag -- unconfined cover concrete
    set IDSteel 4;              # material ID tag – reinforcement
# confined concrete
set fc -200.;           # CONCRETE nominal Compressive Strength (+Tension, -Compression)
set Ec 285000.;         # Concrete Elastic Modulus
# unconfined concrete
set Kfc 1.3;                    # ratio of confined to unconfined concrete strength
set Kres 0.3;                   # ratio of residual/ultimate to maximum stress
set fc1C [expr $Kfc*$fc];       # CONFINED concrete (mander model), maximum stress
set eps1C -0.04
```

```
#set eps1C [expr 2.*$fc1C/$Ec];          # strain at maximum stress
set fc2C [expr $Kres*$fc1C];          # ultimate stress
set eps2C  [expr 3*$eps1C];      # strain at ultimate stress
set lambda 0.1;          # ratio between unloading slope at $eps2 and initial slope $Ec
# unconfined concrete
set fc1U $fc;  # UNCONFINED concrete (todeschini parabolic model), maximum stress
set eps1U -0.003;                    # strain at maximum strength of unconfined concrete
set fc2U [expr 0.2*$fc1U];       # ultimate stress
set eps2U     -0.03;                 # strain at ultimate stress
# tensile-strength properties
set ftC [expr -0.14*$fc1C];       # tensile strength +tension
set ftU [expr -0.14*$fc1U];       # tensile strength +tension
set Ets [expr $ftU/0.012];          # tension softening stiffness
set Fy [expr 3400.];                 # STEEL yield stress
set Es [expr 2100000.];              # modulus of steel
set b 0.01;                          # strain-hardening ratio
# Core concrete (confined)
uniaxialMaterial Concrete02 $IDconcCore $fc1C $eps1C $fc2C $eps2C $lambda $ftC $Ets;
# Cover concrete (unconfined)
uniaxialMaterial Concrete02 $IDconcCover $fc1U $eps1U $fc2U $eps2U $lambda $ftU $Ets;
# build reinforcement material
uniaxialMaterial ReinforcingSteel $IDSteel $Fy 6000  $Es 5000 0.004 0.02 -CMFatigue 0.26 0.506
0.389
set SectionType FiberSection ;       # options: Elastic FiberSection
# define section tags:
set ColSecTagFiber 1;                # assign a tag number to the column section
set BeamSecTagFiber 2;               # assign a tag number to the beam section
# define Beam - Column section geometry
    set HCol 25.;                    # Column Depth
    set BCol 15.;                    # Column Width
    set HBeam 25.;              # Beam Depth
    set BBeam 15.;                       # Beam Width
```

```
    # calculated geometry parameters
    set ABeam [expr $BBeam*$HBeam];
    set IzBeam [expr 1./12.*$BBeam*pow($HBeam,3)];      # Beam moment of inertia
    set ACol [expr $BCol*$HCol];            # cross-sectional area
    set IzCol [expr 1./12.*$BCol*pow($HCol,3)];     # Column moment of inertia
    # FIBER SECTION properties
    # Column section geometry:
    set cover 2.5;                  # rectangular-RC-Column cover
    set numBarsTopCol 2;        # number of longitudinal-reinforcement bars on top layer
    set numBarsBotCol 2;        # number of longitudinal-reinforcement bars on bottom layer
    set numBarsIntCol 2;        # TOTAL number of reinforcing bars on the intermediate layers
    set barAreaTopCol 0.5;      # longitudinal-reinforcement bar area
    set barAreaBotCol 0.5;      # longitudinal-reinforcement bar area
    set barAreaIntCol 0.5;      # longitudinal-reinforcement bar area
    set numBarsTopBeam 2;       # number of longitudinal-reinforcement bars on top layer
    set numBarsBotBeam 2;       # number of longitudinal-reinforcement bars on bottom layer
    set numBarsIntBeam 0;       # TOTAL number of reinforcing bars on the intermediate layers
    set barAreaTopBeam 0.5;     # longitudinal-reinforcement bar area
    set barAreaBotBeam 0.5;     # longitudinal-reinforcement bar area
    set barAreaIntBeam 0.0;     # longitudinal-reinforcement bar area
    set nfCoreY 25;             # number of fibers in the core patch in the y direction
    set nfCoreZ 15;             # number of fibers in the core patch in the z direction
# number of fibers in the cover patches with long sides in the y direction
        set nfCoverY 25;
# number of fibers in the cover patches with long sides in the z direction
    set nfCoverZ 15;
# rectangular section with one layer of steel evenly distributed around the perimeter and a confined
core.
        BuildRCrectSection $ColSecTagFiber $HCol $BCol $cover $cover $IDconcCore
$IDconcCover $IDSteel $numBarsTopCol $barAreaTopCol $numBarsBotCol $barAreaBotCol
$numBarsIntCol $barAreaIntCol  $nfCoreY $nfCoreZ $nfCoverY $nfCoverZ
    BuildRCrectSection $BeamSecTagFiber $HBeam $BBeam $cover $cover $IDconcCore
$IDconcCover $IDSteel $numBarsTopBeam $barAreaTopBeam $numBarsBotBeam
$barAreaBotBeam $numBarsIntBeam $barAreaIntBeam  $nfCoreY $nfCoreZ $nfCoverY $nfCoverZ
```

```
# define geometric transformation: performs a linear geometric transformation of beam stiffness and resisting force from the basic system to the global-coordinate system

    set ColTransfTag 1;                 # associate a tag to column transformation

    set BeamTransfTag 2;                # associate a tag to beam transformation

    set ColTransfType Linear ;          # options, Linear PDelta Corotational

    geomTransf $ColTransfType $ColTransfTag ;     # only columns can have PDelta effects (gravity effects)

    geomTransf Linear $BeamTransfTag  ;

# connectivity:

    set numIntgrPts 10;   #number of integration points for force-based element

    element dispBeamColumn 1 1 3 $numIntgrPts $ColSecTagFiber $ColTransfTag;

    element dispBeamColumn 2 2 4 $numIntgrPts $ColSecTagFiber $ColTransfTag;

    element dispBeamColumn 3 3 4 $numIntgrPts $BeamSecTagFiber $BeamTransfTag;

# Single point constraints -- Boundary Conditions

    fix 1 1 1 1;            # node DX DY RZ

    fix 2 1 1 1;

puts "Model Built"

# define GRAVITY -------------------------------------------------------------

# Slaving a truss node to a beam node where these two nodes are defined at the same location

    equalDOF  5 13 1 2

    equalDOF  6 14 1 2

    equalDOF  7 18 1 2

    equalDOF  8 17 1 2

    equalDOF 9 15 1 2

    equalDOF 10 16 1 2

    equalDOF 11 19 1 2

    equalDOF 12 20 1 2

pattern Plain 1 Linear {

  load 3 0. -10000. 0.;                # node#, FX FY MZ --  superstructure-weight

  load 4 0. -10000. 0.;                # node#, FX FY MZ --  superstructure-weight

}

# Gravity-analysis parameters -- load-controlled static analysis
```

```
set Tol 1.0e-8;                 # convergence tolerance for test
constraints Plain;              # how it handles boundary conditions
numberer Plain;                 # renumber dof's to minimize band-width (optimization), if you want
to
system BandGeneral;             # how to store and solve the system of equations in the analysis
# determine if convergence has been achieved at the end of an iteration step
test NormDispIncr $Tol 6 ;
# use Newton's solution algorithm: updates tangent stiffness at every iteration
algorithm Newton;
set NstepGravity 10;                    # apply gravity in 10 steps
set DGravity [expr 1./$NstepGravity];   # first load increment;
integrator LoadControl $DGravity;       # determine the next time step for an analysis
analysis Static;                        # define type of analysis static or transient
analyze $NstepGravity;                  # apply gravity
# ------------------------------------------------- maintain constant gravity loads and reset time to zero
loadConst -time 0.0
puts "Dusey yukleme ok!"
```

Equivalent Diagonal Struts

Struts

```
# nodal coordinates:
    # For Truss (strut Members)
    model basic -ndm 2 -ndf 2;      # 2 dimensions, 2 dof per node
    node 13 0.1 0.1;
    node 14 199.9 0.1;
    node 17 199.9 137.4
    node 18 0.1 137.4
# Define materials for strut elements
# strut concrete no tensile
```

```
    set matiTag 1
    set fpc -22
    set fpci $fpc;  # concrete compressive strength at 28 days (compression is negative)
    set epsci -0.002;                    # concrete strain at maximum strength
    set fpcui [expr 0.02*$fpci];         # concrete crushing strength
    set epsUi -0.013;                    # concrete strain at crushing strength
        uniaxialMaterial Concrete01 $matiTag $fpci $epsci $fpcui $epsUi
# define GEOMETRY
# HStrut calculated by fema equations
    set HStrut 25
    set BStrut 15
    set AStrut [expr $BStrut*$HStrut];
# Create truss elements - command: element truss trussID node1 node2 A matID
          element truss 14 13 17 $AStrut $matiTag
    element truss 15 14 18 $AStrut $matiTag
```

Links

```
    # nodes for link elements
    node 5 0.1 0.1;
    node 6 199.9 0.1;
    node 7 0.1 137.4;
    node 8 199.9 137.4;
# define elements and sections for link elements
    set LinkSecTag 5;
    set El 30000000;
    set Al 750;
    set Izl [expr 1./12.*15*pow(25,3)];
# Link section
    section Elastic $LinkSecTag $El $Al $Izl;
    set LinkTransfTag 3;
```

```
    geomTransf Linear $LinkTransfTag ;
set numIntgrPts 5;
    element elasticBeamColumn 4 1 5 $Al $El $Izl $LinkTransfTag;
    element elasticBeamColumn 5 2 6 $Al $El $Izl $LinkTransfTag;
    element elasticBeamColumn 6 3 7 $Al $El $Izl $LinkTransfTag;
    element elasticBeamColumn 7 4 8 $Al $El $Izl $LinkTransfTag;
```

Cyclic

```
# execute this file after you have built the model, and after you apply gravity
# source in procedures
source GeneratePeaks.tcl;  # procedure to generate displacement increments for cyclic peaks
# characteristics of cyclic analysis
set IDctrlNode 3;
set IDctrlDOF 1;
set Hload 100;
set iDmax "0.0001 0.00012 0.00018 0.00034 0.00082 0.00178 0.00226 0.0028 0.00328 0.00375
0.00475 0.00726 0.00976 0.0148 0.02 0.025 0.03 0.0349";   # vector of displacement-cycle peaks, in
terms of storey drift ratio
#set iDmax "0.0025 0.005 0.01 0.02 0.025";   # vector of displacement-cycle peaks, in terms of storey
drift ratio
set Fact $LCol ;              # scale drift ratio by storey height for displacement cycles
set Dincr [expr 0.00002*$LCol ];   # displacement increment for pushover. you want this to be very
small, but not too small to slow analysis
set CycleType Full;              # you can do Full / Push / Half cycles with the proc
set Ncycles 1;           # specify the number of cycles at each peak
# -- STATIC PUSHOVER/CYCLIC ANALYSIS
# create load pattern for lateral pushover load coefficient when using linear load pattern
# need to apply lateral load only to the master nodes of the rigid diaphragm at each floor
set iPushNode "3 4";           # define nodes where lateral load is applied in static lateral analysis
pattern Plain 3 Linear {;           # define load pattern -- generalized
    foreach PushNode $iPushNode {
        load $PushNode $Hload 0.0 0.0 0.0 0.0 0.0
```

```
    }
}
# Define DISPLAY ------------------------------------------------------------
#set  xPixels 1200;    # height of graphical window in pixels
#set  yPixels 800;# height of graphical window in pixels
#set  xLoc1 10;    # horizontal location of graphical window (0=upper left-most corner)
#set  yLoc1 10;    # vertical location of graphical window (0=upper left-most corner)
#set ViewScale 2;     # scaling factor for viewing deformed shape, it depends on the dimensions of the model
#DisplayModel3D DeformedShape $ViewScale $xLoc1 $yLoc1  $xPixels $yPixels
#recorder plot $dataDir/DFree.out Displ-X [expr $xPixels+10] 10 300 300 -columns 2 1; # a window to plot the nodal displacements versus time
# ----------- set up analysis parameters
source LibAnalysisStaticParameters.tcl;     # constraintsHandler,DOFnumberer,system-ofequations,convergenceTest,solutionAlgorithm,integrator
#  ---------------------------------     perform Static Cyclic Displacements Analysis
set fmt1 "%s Cyclic analysis: CtrlNode %.3i, dof %.1i, Disp=%.4f %s";     # format for screen/file output of DONE/PROBLEM analysis
foreach Dmax $iDmax {
    set iDstep [GeneratePeaks $Dmax $Dincr $CycleType $Fact];   # this proc is defined above
    for {set i 1} {$i <= $Ncycles} {incr i 1} {
        set zeroD 0
        set D0 0.0
        foreach Dstep $iDstep {
            set D1 $Dstep
            set Dincr [expr $D1 - $D0]
            integrator DisplacementControl  $IDctrlNode $IDctrlDOF $Dincr
            analysis Static
# -----------------------------------------------first analyze command----------------------
            set ok [analyze 1]
# -----------------------------------------------if convergence failure--------------------
            if {$ok != 0} {
    # if analysis fails, we try some other stuff
```

```
# performance is slower inside this loop    global maxNumIterStatic;
      # max no. of iterations performed before "failure to converge" is ret'd
            if {$ok != 0} {
                puts "Trying Newton with Initial Tangent .."
                test NormDispIncr   $Tol 2000 0
                algorithm Newton -initial
                set ok [analyze 1]
            test $testTypeStatic $TolStatic      $maxNumIterStatic  0
                algorithm $algorithmTypeStatic
            }
            if {$ok != 0} {
                puts "Trying Broyden .."
                algorithm Broyden 8
                set ok [analyze 1 ]
                algorithm $algorithmTypeStatic
            }
            if {$ok != 0} {
                puts "Trying NewtonWithLineSearch .."
                algorithm NewtonLineSearch 0.8
                set ok [analyze 1]
                algorithm $algorithmTypeStatic
            }
            if {$ok != 0} {
                set putout [format $fmt1 "PROBLEM" $IDctrlNode $IDctrlDOF [nodeDisp
                $IDctrlNode $IDctrlDOF] $LunitTXT]
                puts $putout
                return -1
            }; # end if
        }; # end if
# --------------------------------------------------------------------------------------------------
        set D0 $D1;             # move to next step
    }; # end Dstep
```

```
    };        # end i

};  # end of iDmaxCycl

# ----------------------------------------------------------------------------------------------------

if {$ok != 0 } {

        puts [format $fmt1 "PROBLEM" $IDctrlNode $IDctrlDOF [nodeDisp $IDctrlNode
        $IDctrlDOF] $LunitTXT]

} else {

        puts [format $fmt1 "DONE"  $IDctrlNode $IDctrlDOF [nodeDisp $IDctrlNode $IDctrlDOF]
        $LunitTXT]

}
```